Drug Design, Development and Therapy Dovepress

Open Access Full Text Article ORIGINAL RESEARCH

Topical hADSCs-HA Gel Promotes Skin Regeneration and Angiogenesis in Pressure Ulcers by Paracrine Activating PPARβ/δ Pathway

Chaoying Jin[1,2,*], Ruolin Zhao[3,4,*], Weihang Hu[5], Xiaolong Wu[4], Li Zhou[6], Letian Shan[4,6], Huiling Wu[1,2]

[1]Department of Plastic and Aesthetic Center, The First Affiliated Hospital, School of Medicine, Zhejiang University, Hangzhou, Zhejiang, 310003, People's Republic of China; [2]School of Medicine, Zhejiang University, Hangzhou, Zhejiang, 310020, People's Republic of China; [3]Yichen Biotechnology Co., Ltd, Hangzhou, Zhejiang, 311200, People's Republic of China; [4]Fuyang Academy, Zhejiang Chinese Medical University, Hangzhou, Zhejiang, 311403, People's Republic of China; [5]Department of Critical Care Medicine, Zhejiang Hospital, Hangzhou, Zhejiang, 310013, People's Republic of China; [6]The First Affiliated Hospital, Zhejiang Chinese Medical University, Hangzhou, Zhejiang, 310060, People's Republic of China

*These authors contributed equally to this work

Correspondence: Letian Shan; Huiling Wu, Email letian.shan@zcmu.edu.cn; zywhl@zju.edu.cn

Background: Pressure ulcer is common in the bedridden elderly with high mortality and lack of effective treatment. In this study, human-adipose-derived-stem-cells-hyaluronic acid gel (hADSCs-HA gel) was developed and applied topically to treat pressure ulcers, of which efficacy and paracrine mechanisms were investigated through in vivo and in vitro experiments.

Methods: Pressure ulcers were established on the backs of C57BL/6 mice and treated topically with hADSCs-HA gel, hADSCs, hyaluronic acid, and normal saline respectively. The rate of wound closure was observed continuously during the following 14 days and the wound samples were obtained for Western blot, histopathology, immunohistochemistry, and proteomic analysis. Human dermal fibroblasts (HDFs) and human venous endothelial cells (HUVECs) under normal or hypoxic conditions were treated with conditioned medium of human ADSCs (ADSC-CM), then CCK-8, scratch test, tube formation, and Western blot were conducted to evaluate the paracrine effects of hADSCs and to explore the underlying mechanism.

Results: The in vivo data demonstrated that hADSCs-HA gel significantly accelerated the healing of pressure ulcers by enhancing collagen expression, angiogenesis, and skin proliferation. The in vitro data revealed that hADSCs strengthened the proliferation and wound healing capabilities of HDFs and HUVECs, meanwhile promoted collagen secretion and tube formation through paracrine mode. ADSC-CM was also proved to exert protective effects on hypoxic HDFs and HUVECs. Besides, the results of proteomic analysis and Western blot elucidated that lipid metabolism and PPARβ/δ pathway mediated the healing effect of hADSCs-HA gel on pressure ulcers.

Conclusion: Our research showed that topical application of hADSCs-HA gel played an important role in dermal regeneration and angiogenesis. Therefore, hADSCs-HA gel exhibited the potential as a novel stem-cell-based therapeutic strategy of treating pressure ulcers in clinical practices.

Keywords: pressure ulcer, wound healing, human adipose derived stem cell, hydrogel, PPARβ/δ, lipid metabolism, skin regeneration

Introduction

Pressure ulcers are defined as localized injuries in the skin and underlying soft tissues as a result of prolonged pressure or pressure in combination with friction and shearing force.[1] Multiple factors contribute to the pathophysiology of pressure ulcers, among which hypoxia plays a major role.[2,3] In chronic wounds represented by pressure ulcers, severe damage of the vascular network obstructs oxygen supply, which inhibits extracellular matrix (ECM) synthesis, angiogenesis and re-epithelialization.[4,5] Besides, persistent hypoxia also increases the production of reactive oxygen species (ROS), which exacerbates inflammation and prolongs the healing of wounds.[6,7] As a refractory disease causing about 1 to 3 million

Received: 27 May 2024
Accepted: 9 October 2024
Published: 26 October 2024

Graphical Abstract

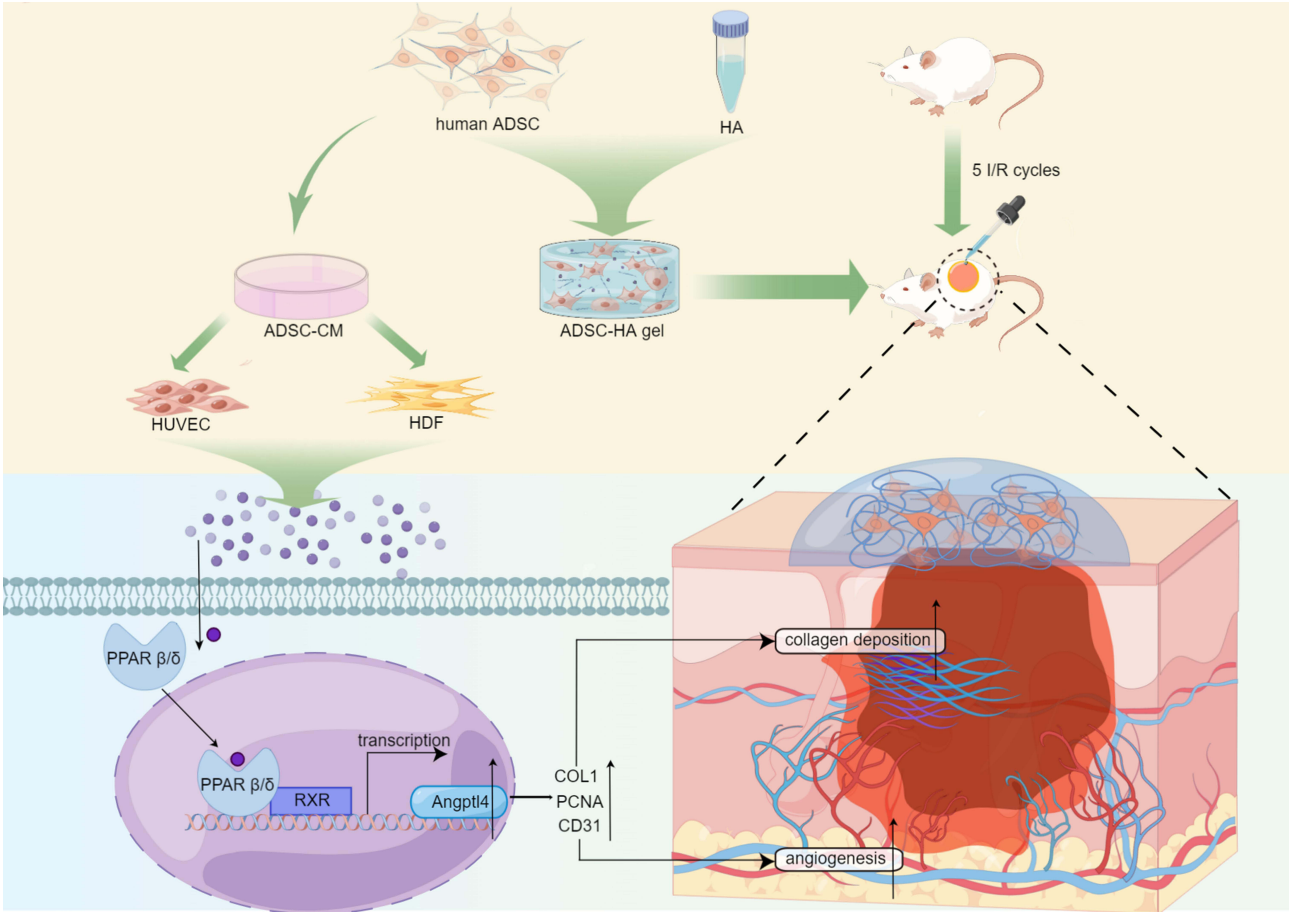

death annually in the United States, pressure ulcers not only exert negative impacts on the life quality of patients in physical, social, and psychological aspects, but also lead to increased mortalities in both acute and long-term care settings.[8–13] Conventional treatments for pressure ulcers include negative-pressure wound therapy, air-fluidized therapy, ultrasound therapy, electromagnetic therapy, and surgical flap grafting.[14–16] Recently, some novel methods have been developed to accelerate wound healing, such as growth factors supplementation, somatic cell therapy, and skin tissue engineering.[17–19] However, the clinical outcomes remain unsatisfactory and radical therapy is in urgent need. To take a step forward in innovative ways to improve the treatment of pressure ulcers, our study developed a novel approach to topically deliver human adipose-derived stem cells (hADSCs) in hyaluronic acid (HA) which is termed as hADSCs-HA gel.

hADSCs, a class of mesenchymal stem cells (MSCs) that are abundant and easy to extract, have been widely recognized to promote wound healing.[20] Earlier studies have reported that hADSCs have multidirectional differentiation potential and can directly participate in wound repair by differentiating into skin cells, vascular endothelial cells, etc.[21,22] However, recent evidence suggests that the main mechanism by which hADSCs aid in wound healing is mainly based on their paracrine nature, that is, the secretion of multiple bioactive molecules comprised of various growth factors, cytokines, and chemokines. hADSCs modulate the inflammatory responses at the wound site by secreting anti-inflammatory cytokines and promoting macrophage polarization from M1 to M2.[23] In addition, hADSCs support the formation of new vessels by secreting a variety of pro-angiogenic factors such as VEGF, PDGF, FGF-2, and IGF-1, thus enhancing blood supply to the wound.[24] Besides, hADSCs paracrinally facilitate the proliferation and migration of the participant

cells in wound repair, such as human dermal fibroblasts (HDFs), human umbilical vein endothelial cells (HUVECs), and human keratinocytes (HaCaTs), which stimulates wound healing.[25–28] hADSCs can also release a range of matrix metalloproteinases (MMPs) that, through inducing the breakdown, remodeling, and regeneration of the extracellular matrix (ECM), enhance wound mechanics and facilitate tissue recovery.[29] In clinical trials, transplantation of hADSCs has been used as a therapeutic approach for limb ischemia, diabetic ulcers, and burns.[30–34] Animal studies have revealed that hADSCs could improve the healing of pressure ulcers in both young and old mice, which were further confirmed with both fresh and cryopreserved hADSCs.[35,36] These clinical and preclinical studies suggest that hADSCs are suitable candidates for treating pressure ulcers.

HA is a polysaccharide that exists naturally in the ECM of human body. Because of its excellent moisturizing, lubricating, biocompatible and biodegradable properties, it has a wide range of applications in wound treatments.[37] By absorbing and maintaining water, HA promotes wound hydration, shields the wound from harmful substances, and accelerates epithelial regeneration.[38] HA can also interact with CD44 to reduce the recruitment of inflammatory cells and alleviate tissue damage.[39] Besides, with the ability to bind with RHAMM, HA contributes to the formation of new vessels and the migration of HDFs and HUVECs.[40,41] By stimulating collagen synthesis by HDFs, HA also participates in the synthesis and remodeling of ECM, which enhances the strength and elasticity of newly formed tissue.[42] Notably, prior research has demonstrated that HA promotes stem cell migration and differentiation, encourages their aggregation towards the wound site, and has a good synergistic effect on the biological function of stem cells in treating wounds.[43] Therefore, HA is widely used as a scaffolding material in tissue engineering to support cell proliferation and tissue regeneration.[44]

Compared with previously reported techniques, hADSCs-HA gel presents significant advantages in the treatment of pressure ulcers. For instance, though surgical debridement therapy removes dead tissue and leaves wound beds clean, it also entails risks of bleeding, infection, discomfort, and anesthetic complications.[45] Negative pressure wound therapy (NPWT), while promoting drainage of exudate from the wound site, has limited efficacy in the management of large or deep ulcers and may increase discomfort.[46] While ultrasonic therapy can increase blood flow and boost cell activity, its efficacy varies depending on frequency and intensity of treatment and may cause thermal damage to adjacent tissues.[47] In contrast, hADSCs-HA gel can be applied directly to the wound without the need for invasive surgeries or complex manipulations, thus minimizing patient discomfort and infection risk. More importantly, in addition to being loaded with hADSCs that can paracrinally stimulate wound healing, hADSCs-HA gel is further innovated and optimized in the delivery of stem cells. Current applications of hADSCs in wound healing are mainly based on systematic administration and local delivery.[48] Systematic administration is confronted with high cellular reduction rate and the difficulty in precise tissue targeting.[49] Therefore, local delivery is gaining increasing interest particularly in the large surface area wounds and chronic non-healing wounds. Local approaches mainly include subcutaneous injection and topical application. However, shear injury during injection has a negative effect on cell engraftment rate.[50] Alternatively, topical applications of hADSCs could avoid these issues. For instance, 3D keratin scaffolds supported the adhesion, proliferation, and differentiation of hADSCs. It also aided hADSCs to promote wound healing and remodeling in vivo.[51] To enhance the therapeutic efficacy of hADSCs, several scaffolds have been developed to facilitate the delivery and survival of hADSCs, such as biodegradable albumin scaffold, carboxymethyl cellulose hydrogel, and poly vinyl alcohol hydrogel.[52–54] HA is a natural polymer present in the connective, epithelial, and neural tissues and is also a substantial constituent of extracellular matrix (ECM).[55] Because of its high molecular weight, hydrophilic nature, and biocompatibility characteristics, HA acts as a promising cellular scaffold which can promote the survival and biological activity of hADSCs.[56–59] Several studies have demonstrated that by applying the hydrogel containing hADSCs and HA topically, the healing of burn wounds, radiation injuries, and diabetic ulcers can be accelerated with promoted re-epithelization and angiogenesis.[60–62] However, topical applications of such hydrogel on pressure ulcers have been rarely reported.

In this study, in vivo effects of hADSCs-HA gel were evaluated on a mouse pressure ulcer model by skin histopathological and immunohistochemical analyses. The paracrine effect of hADSCs was further investigated at the cellular level by employing conditioned medium of hADSCs (ADSC-CM) on HDFs and HUVECs under both normal and hypoxic conditions. Also, we explored the underlying mechanism with the aid of proteomic analysis. The fundamental innovation and benefit of our findings is that we offer a minimally invasive method for applying hADSCs to pressure ulcers, which enables highly efficient and safe applications of hADSCs in clinical settings.

Methods

Reagents and Chemicals

Alpha Minimal Essential Medium (α-MEM), High D-Glucose Dulbecco's Modified Eagle Medium (DMEM), premium fetal bovine serum (premium FBS), trypsin (0.25%), and phosphate buffered saline (PBS) were purchased from Gibco BRL (NY, USA). Fetal bovine serum (FBS) was purchased from CellMax (Beijing, China). Cell culture plates were purchased from Eppendorf (Hamburg, Germany). Pentobarbital sodium (1030001) was purchased from Sigma-Aldrich (USA). Radioimmunoprecipitation assay (RIPA) buffer and proteinase inhibitor cocktails were purchased from Bimake (TX, USA). Hyaluronic acid (HA) powder (H909938) was bought from Macklin (Shanghai, China). Medical recombinant type III humanized collagen gel was purchased from Newliann (Hunan, China). Magnetic plates weighing about 2.5 g with a 12-mm diameter, a 3-mm thickness and a 1000 G magnetic force were purchased from Minci (Shenzhen, China). Masson staining kit (R20381) was obtained from Yuanye (Shanghai, China). Bicinchoninic acid (BCA) protein quantification kit was bought from Thermo (USA). Antibody of β-actin (A3854) was purchased from Sigma-Aldrich (USA). Antibodies of COL1 (A16891) and PPARβ/δ (A5656) were bought from Abclonal (Wuhan, China). Antibody of COL3 (NB600-594) was purchased from Novus (Shanghai, China). Antibody of PCNA (13110) were bought from Cell Signaling Technology (MA, USA). Monoclonal antibody of CD31 (3528) was bought from Cell Signaling Technology (MA, USA). Polyclonal antibody of CD31 (YP-Ab-16944) was bought from UpingBio Technology (Shenzhen, China). Antibody of ANGPTL4 (18374-1-AP) was purchased from Proteintech (Wuhan, China). Antibody of HIF-1α (WL01607) was purchased from Wanleibio (Shenyang, China). Cobalt chloride hexahydrate ($CoCl_2$, C116457) was purchased from Aladdin (Shanghai, China). Nitrocellulose membrane was bought from Sartorius Stedim Biotech (Göttingen, Germany). Western Lightning® Plus ECL was obtained from Biosharp (Beijing, China). Cell counting kit-8 (CCK-8, B34304) was bought from Bimake (TX, USA). GSK3787 (S8025) was purchased from Selleck (Shanghai, China).

Animal Preparation

All animal experimental procedures were performed according to the guidelines for the Care and Use of Laboratory Animals of the National Institutes of Health and were approved by the Medical Norms and Ethics Committee of Zhejiang Chinese Medical University (grant number: 20210705–12). Male C57BL/6 mice (8-week-old), weighing about 30 g, were provided by Shanghai Slack Company, animal production license number (SCXK: 2017–0005 Shanghai, Zhejiang, China). The mice were quarantined for one week before being kept in the Animal Experimental Research Center of Zhejiang Chinese Medical University with ad libitum access to water and chow on a 12 h light: 12 h dark cycle.

Culture of hADSCs, HDFs, and HUVECs and Preparation of hADSCs-HA Gel

The primary hADSCs (PZF21000003) were provided by Hangzhou Regional Cell Preparation Center and were subjected to quality control by being tested for bacteria, fungi, mycoplasma, virus contamination, and specific markers of stem cells. The cells were maintained in α-MEM supplemented with 10% premium FBS and were cultured at 37 °C with 5% CO_2. The cells at passage 5 were used for the preparation of hADSCs-HA gel and conditioned medium of ADSC (ADSC-CM). The HDF (KCB200537) and HUVEC (KCB 2010233YJ) cell lines were provided by Kunming Cell Bank of Chinese Academy of Sciences and were cultured in DMEM with 10% FBS at 37 °C with 5% CO_2.

HA powder was dissolved in saline at a concentration of 6 mg/mL. hADSCs were cultivated to the 5th generation and reached 90% confluence before being harvested by 0.25% trypsin. After the centrifugation at 1000 rpm for 5 min, the hADSCs were re-suspended by the HA solution at a concentration of 10^4 cells/μL to obtain hADSCs-HA gel.

Animal Modeling and Treatment

A total of 32 C57BL/6 mice were employed to evaluate the therapeutic effects of hADSCs-HA gel on the pressure ulcer. As previously reported, the pressure ulcer model was established on the mice back.[63–66] Briefly, after being anesthetized by an intraperitoneal injection of 50 mg/kg pentobarbital sodium, the mice back were depilated and sterilized. Then the dorsal skin was gently pulled up and pinched between two circular magnetic plates for 12 hours, followed by a 12-hour rest period, to simulate an ischemia-reperfusion (I/R) cycle. Totally, 4 I/R cycles were performed in 4 days, and the pressure ulcer formed after the last I/R cycle. Then the 32 mice were equally randomized into 4 groups (n = 8): model

group, HA group, ADSC group, and hADSCs-HA gel group. In the hADSCs-HA gel group, 200 μL hADSCs-HA gel was topically applied using syringes onto the wound beds of mice once every other day. hADSCs were suspended in saline at the concentration of 10^4 cell per μL and 200 μL of such solution was applied topically with syringes on the wounds of mice in the ADSC group. HA powder was dissolved in saline at the concentration of 6 mg per mL and the wounds of mice in the HA group were treated with 200 μL HA solution topically using syringes. In the model group, topical application of 200 μL saline was conducted with syringes on the pressure ulcers of mice.

In another parallel experiment, we compared the therapeutic efficacy of hADSCs-HA gel and a commercially available medical recombinant type III humanized collagen gel. After undergoing the same approach of modeling, 40 mice were equally randomized into 5 groups (n = 8): model group, HA group, ADSC group, hADSCs-HA gel group, and collagen group. The mice in the collagen group were treated with 200 μL collagen gel topically and the other 4 groups received the same treatment as mentioned above.

Throughout the 2-week trial period, the ulcer wound area was checked daily and the images of the wound sites were taken every 4 days. The wound closure rate was measured using the Image J 1.47 software (Version: 1.6.0) (Media Cybernetics, Bethesda, MD, USA) according to the formula: wound closure rate (%) = $(A_0 - A_t) / (A_0) \times 100\%$, in which A_0 was the original wound area and A_t was the wound area at the indicated times.

Histopathological Observation

The mice were sacrificed on the 14th day and approximately 3 mm thickness of full-layer traumatic tissue samples were harvested along the outer edge of the entire wound. After fixed in 4% paraformaldehyde for 48 hours at room temperature, the skin samples were dehydrated through a series of graded ethanol, embedded in paraffin, and then cut into 3-μm-thick sections. The slices were stained with hematoxylin and eosin (H&E) and scanned with a microscope (Axio Scope A1, ZEISS, Germany). The analysis of histological structure and wound width was conducted with the Image J 1.47 software (version: 1.6.0). Masson staining was carried out using commercial staining kits according to the manufacturer's instructions. Photographs were captured by the microscope and were analyzed for collagen deposition with the Image J 1.47 software (version: 1.6.0) based on the amount of blue staining in relation to the overall area of the photomicrographed tissue.

Immunohistochemical Analysis

Immunohistochemistry was performed according to the previous reports.[67,68] Briefly, after the sections were rehydrated and blocked, they were incubated with primary antibodies overnight at 4 °C. The primary antibodies were as follows: Col-1 (1:200), Col-3 (1:200), CD31 (1:800), and PCNA (1:4000). After the application of corresponding secondary antibodies, the DAB substrate was used to detect antibody binding. Finally, after being counterstained with hematoxylin, the slides were pictured using a fluorescence microscope and the positive areas were measured using the Image J 1.47 software (version: 1.6.0).

Proteomic Analysis of Mice Skin Samples

Preparation of Protein Samples and LC-MS/MS Analysis

When the mice from the model group, the HA group and the hADSCs-HA group were sacrificed on the 14th day, replicated skin samples were taken from the wound sites and put on ice immediately. After adding protein lysate (8 M urea, 1% SDS), which contained protease inhibitor to inhibit protease activity, the mixture was treated by ultrasound for 2 min at a low temperature, followed by splitting for 30 min. After centrifugation at 12000 g at 4 °C for 30 min, the concentration of protein supernatant was determined by BCA protein quantification assay. Peptides were got after the protein samples were digested and they underwent LC-MS/MS analysis by an EASY nLC-1200 system (Thermo, USA) coupled with a timsTOF Pro2 (Bruker, Germany) mass spectrometer at Majorbio Bio-Pharm Technology Co. Ltd. (Shanghai, China).

Bioinformatics Analyses

The raw files from LC-MS/MS spectra were imported into the MaxQuant version 2.0.3.1 software system for database searching analysis. The databases used are mainly the NCBI, UniProt databases for specified species protein sequences

and other species libraries such as self-measured genomes, transcriptome data, species-specific databases, etc. Protein differential expression analysis among the three identified protein groups was performed with R software (R4.0.1, the EDGER package). Differences were tested by Welch analysis with thresholds of $|\log2FC| \geq 0.263$ and $p < 0.05$. To draw volcano plot, the change fold of protein expression difference was used as X ais and p value was used as Y-axis. The values of the horizontal and vertical coordinates were logarithmically processed. Venn analysis was conducted with the software developed by Majorbio to provide a visual presentation of the number of proteins in each protein set and the overlaps between them. Expression pattern clustering analysis was performed based on information about protein expression in different samples by calculating the distance between proteins and then classifying the proteins with an iterative approach. Blast2GO 2.5.0 was applied in the GO enrichment analysis according to biological processes, cellular components and molecular functions. We also used the GO enrichment string diagram to show the correspondence between the target proteins and the GO terms. KEGG analysis was conducted with KOBAS software to display the KEGG pathways which the differential proteins participated in.

In vitro Experiments

In vitro experiments were conducted to determine the effects of ADSC-CM on HDFs and HUVECs. DMEM with 10% FBS culturing HDFs or HUVECs for 48 h was collected as the culturing medium of HDFs (HDF-CM) or the culturing medium of HUVECs (HUVEC-CM) respectively. hADSCs were switched to DMEM with 10% FBS and incubated for 48 h to get the conditioned medium of hADSCs (ADSC-CM).

HDFs and HUVECs were divided into 2 groups to determine the effects of ADSC-CM under normal conditions: normal control (NC) group and ADSC-CM group. NC group was treated by HDF-CM or HUVEC-CM and ADSC-CM group was treated by ADSC-CM at the same concentration. With the same intervention span, the 2 groups underwent CCK-8, wound healing, and tube formation assays. After 48 h treatment, protein was extracted for Western blot.

HDFs and HUVECs were divided into 3 groups to determine the effects of ADSC-CM on hypoxic cells: NC group, Hypoxia group, and Hypoxia + ADSC-CM group. The NC group was cultured with HDF-CM or HUVEC-CM. The Hypoxia group was treated with 100 μM $CoCl_2$ in HDF-CM or HUVEC-CM and the Hypoxia + ADSC-CM group was treated with 100 μM $CoCl_2$ in ADSC-CM. With the same intervention span, the 3 groups underwent wound healing. After 48 h treatment, protein was extracted for Western blot.

GSK3787, which is a selective and irreversible inhibitor of PPARβ/δ, was used to verify the PPARβ/δ mechanism. HDFs and HUVECs were seeded into 10 cm plates and divided into 4 groups respectively: NC group, GSK3787 group, ADSC-CM group and ADSC-CM + GSK38787 group. The NC group was treated with HDF-CM or HUVEC-CM. The GSK3787 group was treated with GSK3787 at the concentration of 1 nM. The ADSC-CM group was treated with ADSC-CM and the ADSC-CM + GSK3787 group was treated with ADSC-CM supplemented with 1 nM GSK3787. After 48 h intervention, total proteins of each group were extracted for Western blot analysis.

Cell Proliferation Assay

The proliferation of HDFs was measured with CCK-8. HDFs (2.5×10^3 cells per well) were seeded into 96-well plates and were divided into two groups: normal control group (NC) and ADSC-CM group. HDF-CM was used to dilute the ADSC-CM at the gradient of 20%, 40%, 60%, and 80%. DMEM with 10% FBS culturing HDFs for 48 h was collected as the culturing medium of HDFs (HDF-CM). hADSCs were switched to DMEM with 10% FBS and incubated for 48 h to get the conditioned medium of hADSCs (ADSC-CM). The ADSC-CM groups were treated with different concentrations of ADSC-CM, while the HDF-CM was applied to the NC group. After 24 h of treatment, 10 μL of CCK-8 reagent was added to each well of the culture medium (100 μL per well), and the absorbance of each well was observed at 450 nm using a microplate reader (Bio-Rad 680, Hercules, USA). The proliferation of HUVECs was measured using the same kit as mentioned above. HUVECs were seeded in the 96-well plate at a density of 3×10^3 cells per well. DMEM with 10% FBS culturing HUVECs for 48 h was collected as the culturing medium of HUVECs (HUVEC-CM) and the same treatment approach was followed. After 48 h of treatment, the absorbance at 450 nm was measured. For each experiment, 3 biological replicates were performed.

Wound Healing Assay

HDFs were cultivated to reach 100% confluence after being seeded in 6-well plates at a density of 1.5×10^5 cells per well. The HDFs were then divided into two groups: the NC group and the ADSC-CM group. The culture medium was discarded, and artificial wounds were made in each well using 200 μL pipette tips. The width of each scratch was kept consistent and measured as the baseline value. The ADSC-CM was diluted 10-fold with FBS-free DMEM to eliminate the effect of FBS on cell proliferation. At the same time, HDF-CM was also diluted 10-fold with FBS-free DMEM. The wells of the NC group and the ADSC-CM group were then washed with PBS and supplemented with diluted HDF-CM and ADSC-CM respectively. Then the cells were cultured for 0 h, 24 h and 48 h in a 5% CO_2 incubator during which the width of the scratch was observed with an inverted microscope (CarlZeiss, Göttingen, Germany) and measured by the Image J 1.47 software (version: 1.6.0). The closure percentage of the scratch was calculated as below: wound healing rate (%) = $(A_0 - A_t) / A_0 \times 100\%$. A_0 represented the initial wound area and A_t represented the remaining wound area when the measurement was done. The wound healing ability of HUVECs was evaluated in the same way as HDFs and the dynamic observation of the scratches was done at 0 h, 24 h, 48 h and 72 h after treatment.

To investigate the effects of ADSC-CM under hypoxic conditions, the artificial wounds in the NC group were cultured in diluted HDF-CM or HUVEC-CM. The Hypoxia group was treated with 100 μM $CoCl_2$ in diluted HDF-CM or HUVEC-CM, while the Hypoxia + ADSC-CM group was treated with 100 μM $CoCl_2$ in diluted ADSC-CM. The width of wounds was observed and calculated at 0 h, 24 h, and 48 h with the same method as mentioned above. For each experiment, 3 biological replicates were performed.

Tube Formation Assay

HUEVCs (1×10^5 cells per well) were seeded on a Matrigel-coated plate. Then the cells in the NC group and the ADSC-CM group were treated with HUVEC-CM and ADSC-CM respectively. Images were taken using an inverted microscope following 0 h, 2 h, 4 h, and 6 h of incubation at 37 °C with 5% CO_2. To evaluate the tube formation properties of HUVECs in different groups, the number of branching points and the total tube length were calculated with the Image J 1.47 software (version: 1.6.0). For each experiment, 3 biological replicates were performed.

Western Blot Analysis

After the total proteins of mice skin samples, HDFs and HUVECs were extracted with RIPA lysis buffer supplemented with proteinase inhibitor, they were quantified with the BCA protein quantification assay. The protein samples were then separated by denaturing sodium dodecyl sulfate polyacrylamide gel electrophoresis (SDS-PAGE; 6~12%) and transferred onto nitrocellulose membranes. The membranes were blocked with 5% non-fat milk for 1 h at room temperature and incubated at 4 °C with primary antibodies. The primary antibodies were as follows: PPARβ/δ (1:1000), ANGPTL4 (1:1000), COL1 (1:1000), PCNA (1:1000), CD31 (1:1000), and HIF-1α (1:1000). β-actin (1:20000) served as a control. After being washed, the membranes were incubated with peroxidase-conjugated secondary antibodies at 4 °C for 2 h. Finally, all the proteins bands were detected by ECL kit and visualized by GE ImageQuant LAS4000 System 1 (Bio-Rad, Hercules, CA, USA). Results were analyzed with the Image J 1.47 software (version: 1.6.0). For each experiment, 3 biological replicates were performed.

Statistical Analysis

Data were expressed with the form of mean ± standard deviation (SD). GraphPad prism 9 (version: 9.5.1) was adopted to process the data and one-way ANOVA analysis was used to compare the data from different groups. A p value < 0.05 is considered as significant and a p value < 0.01 is considered as very significant.

Results

hADSCs-HA Gel Accelerated Wound Healing of Pressure Ulcers in vivo

To evaluate the in vivo effects of hADSCs-HA gel on skin pressure ulcers, the dorsal wounds of pressure ulcers in mice were photographed following treatments from day 2 to day 14. As shown in Figure 1A and F, the wound closure rate was

significantly increased following topical treatments of HA, hADSCs, and hADSCs-HA gel on the wounds of mice (all $p <$ 0.01 vs model). Surprisingly, the pressure ulcers in the ADSC-HA group healed more quickly than the other 2 treatment groups, reaching a 96.91% ± 1% closure on day 14, compared to 88.20% ± 0.36% in HA group, and 86.72% ± 0.63% in ADSC group ($p < 0.05$ or $p < 0.01$ vs ADSC-HA). As shown in SFigure 1A and C, the wound closure rate was significantly higher in the ADSC-HA group than that in the collagen group at days 6, 10, and 14 (all $p < 0.01$ vs collagen).

Histopathological analysis was conducted on wound samples of mice by HE and Masson staining. As shown in Figure 1B and G, the maximal diameter of the wound in the model group was considerably larger than that in the other three groups (all $p < 0.01$). By contrast, the diameter of wounds in the ADSC-HA group was significantly smaller compared to the HA and ADSC groups (both $p < 0.01$). According to the detailed skin structure presented in Figure 1C, the squamous epithelium in the model group was necrotic and detached. In the dermis of the model group, large areas of inflammatory cell infiltration were visible and the fibrous arrangement was greatly disordered. In comparison to the model group, the HA and ADSC groups showed signs of partial skin repair, including a modest degree of normal squamous epithelial regeneration, decreased inflammatory necrotic exudate, and decreased inflammatory cell infiltration.

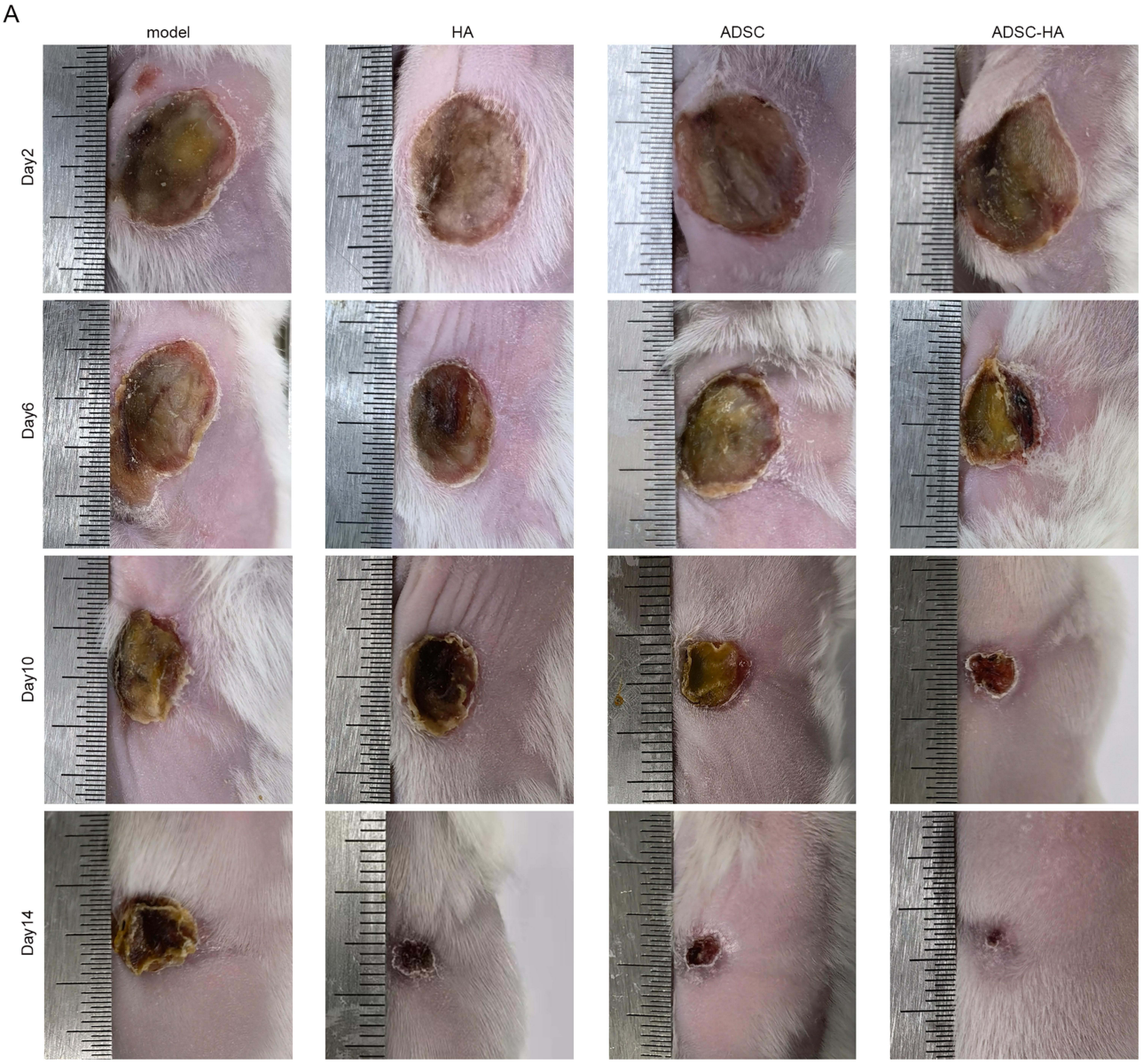

Figure 1 Continued.

In the ADSC-HA group, there was obvious regeneration of normal squamous epithelium. The granulation and fibrous tissue regenerated significantly in the dermis with increased amounts of fibroblasts and normal hair follicles, indicating finely restored skin structure with the treatment of hADSCs-HA gel. Figure 1D showed high magnification of angiogenic areas. In the model group, a small number of neovessels was visible in the dermis with discontinuous fibrous walls. In the HA group, a small amount of neovascularization was randomly and independently distributed within the hyperplastic fibrous tissue. In the ADSC group, plenty of neovessels were seen in the dermis and surrounded by mixed infiltrate of neutrophils and macrophages. In the ADSC-HA group, a significant number of neovasculature was distributed in clusters, most of which were morphologically naive surrounded with ferritin-containing macrophages. As shown in Figure 1E and H, the Masson staining results revealed that collagen production was promoted in both ADSC ($p < 0.05$) and ADSC-HA groups ($p < 0.01$) compared to the model group. Meanwhile, the positive area of collagen fibers in the ADSC-HA group was larger than that in the HA and the ADSC group ($p < 0.05$ vs HA, $p < 0.01$ vs ADSC). Taken together, the above results indicated that hADSCs-HA gel accelerated the healing of pressure ulcers by promoting the restoration of skin structure, which outperformed topical treatments of HA, hADSCs or commercial collagen gel alone.

hADSCs-HA Gel Enhanced Collagen Expression, Angiogenesis, and Skin Proliferation of Pressure Ulcers in vivo

Immunohistochemistry of Col-1 and Col-3 was performed to obtain insights into the collagen architecture in response to the hADSCs-HA gel treatment. As shown in Figure 2A–D, the expressions of skin Col-1 and Col-3 significantly increased after topical treatments of HA, hADSCs, and hADSCs-HA gel on the dorsal skin wounds of mice (Col-1: all $p < 0.01$; Col-3: $p < 0.05$ or $p < 0.01$ vs Model). Of note, hADSCs-HA gel gave rise to higher expressions of Col-1 and Col-3, compared to the HA and the ADSC groups (Col-1: $p < 0.05$ or $p < 0.01$ vs ADSC-HA; Col-3: both $p < 0.01$ vs ADSC-HA).

Pro-angiogenic and pro-proliferative effects of hADSCs-HA in vivo were conducted via CD31 and PCNA immunohistochemistry, respectively. As shown in Figure 2E–H, the skin CD31 and PCNA expressions were significantly

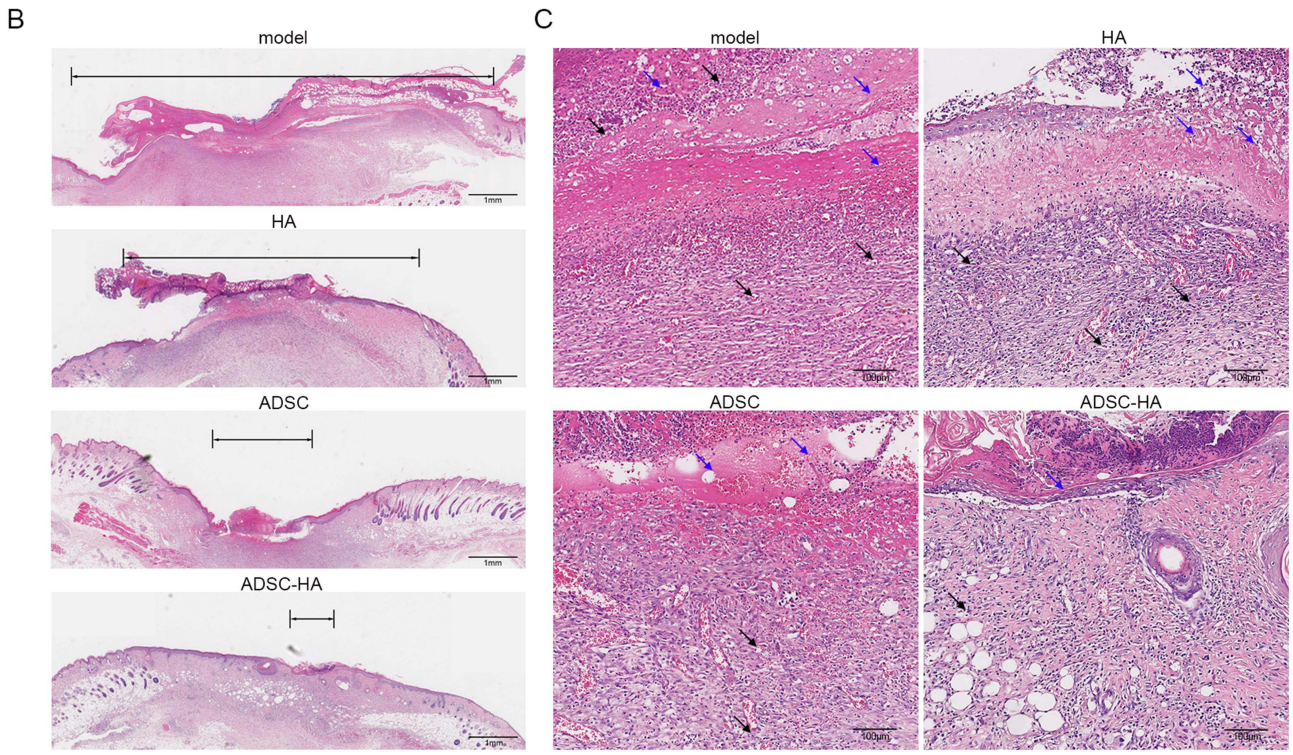

Figure 1 Continued.

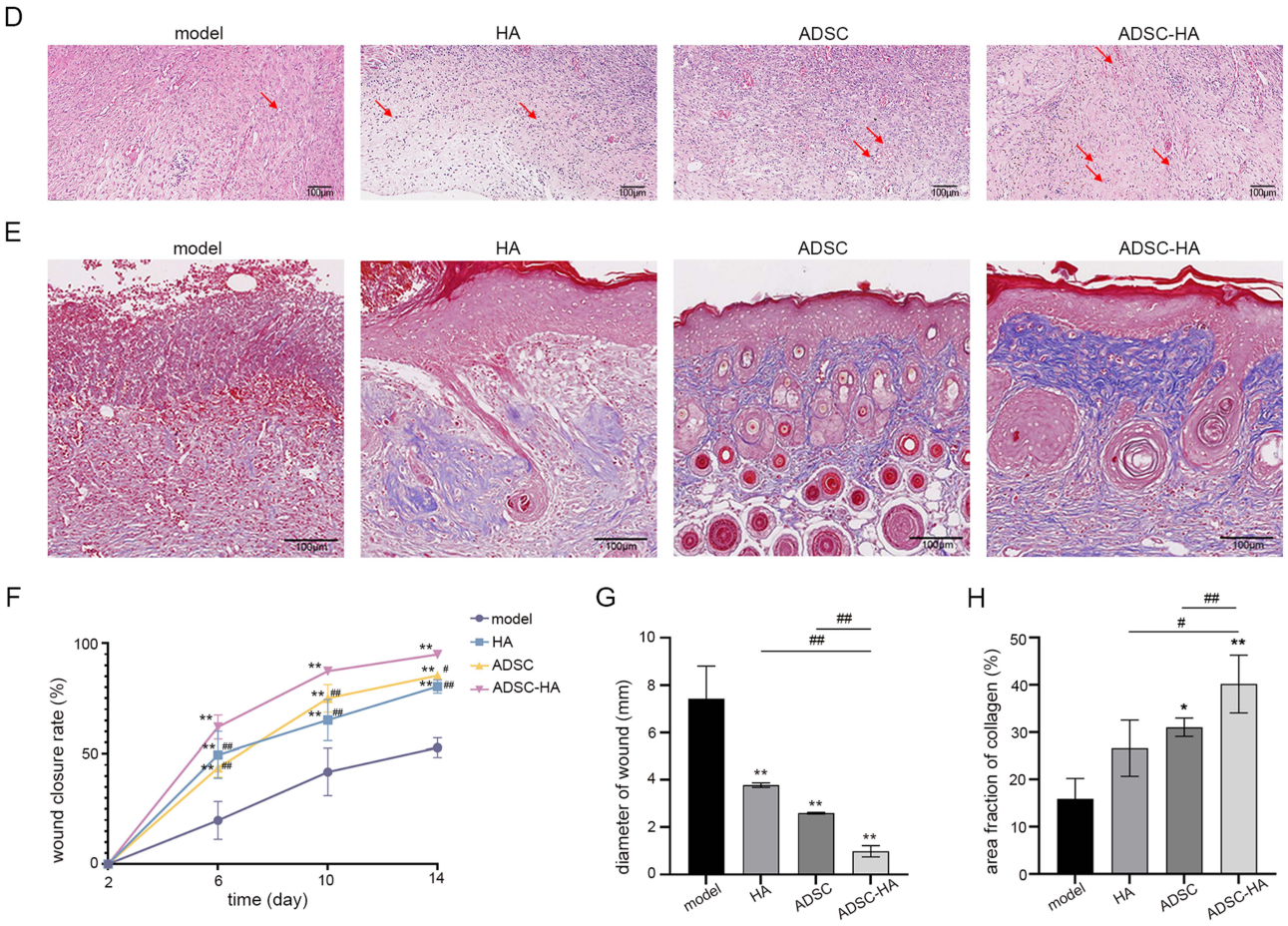

Figure 1 The effects of human ADSCs-hyaluronic acid (hADSCs-HA) gel on pressure ulcers in vivo. (**A**) Representative images of dorsal skin wounds in mice recorded at 2, 6, 10, and 14 days after topical applications of saline (model), hyaluronic acid (HA), hADSCs (ADSC) or hADSCs-HA gel (ADSC-HA). (**B**) Hematoxylin-eosin (HE) staining of the wound areas on day 14 (scale bar = 1 mm). (**C**) High magnification view of HE stained skin structures at wound sites (10X, scale bar = 100 μm). Black arrows highlight inflammatory cells. Blue arrows highlight necrotic exudate. (**D**) High magnification view of HE stained angiogenic areas (20X, scale bar = 100 μm). Red arrows highlight neovascularization. (**E**) Masson staining of the wound areas on day 14 (scale bar = 100 μm). (**F**) Quantification of the wound closure rate according to the formula: wound closure rate (%) = $(A_0 - A_t) / (A_0) \times 100\%$. A_0 was the original wound area and A_t was the wound area at the indicated times. (**G**) Quantification of the diameter of wounds on day 14 evaluated by HE staining. (**H**) Quantification of the area fraction of collagen on day 14 evaluated by Masson staining. Data are shown as mean ± SD (n = 5); $^{*}p < 0.05$ vs model, $^{**}p < 0.01$ vs model; $^{\#}p < 0.05$ vs ADSC-HA, $^{\#\#}p < 0.01$ vs ADSC-HA.

elevated after topical treatments of HA, hADSCs, and hADSCs-HA gel on the dorsal skin wounds of mice ($p < 0.05$ or $p < 0.01$ vs model). Furthermore, the positive areas of CD31 and PCNA in the ADSC-HA group were significantly larger than that of the HA and the ADSC groups ($p < 0.05$ or $p < 0.01$ vs ADSC-HA).

Western blot was also conducted to further present the quantitative expression of Col-1, CD31, and PCNA in mice skin. As shown in Figure 2I–L, the Col-1, CD31, and PCNA expressions in the ADSC group and ADSC-HA group were significantly increased ($p < 0.05$ or $p < 0.01$ vs model). Notably, the results of Western blot also indicated that ADSC-HA gel significantly increased the expressions of Col-1, CD31, and PCNA than hADSCs or HA alone ($p < 0.05$ or $p < 0.01$ vs ADSC-HA). The data in SFigure 1B, D, E and F showed that Col-1, CD31 and PCNA in the ADSC-HA group were all significantly higher than that in the collagen group (all $p < 0.01$ vs. collagen.

The above data suggested that hADSCs-HA gel could facilitate wound healing by promoting collagen deposition, enhancing vessel regeneration, and improving cell proliferation in vivo at the pressure ulcer site.

ADSC-CM Promoted the Proliferation, Wound Healing Ability, and Collagen Secretion of HDFs in vitro

Wound healing, CCK-8, and Western blot assays were conducted to investigate the pro-migrative, proliferative, and collagen-promoting effects of ADSC-CM on HDFs. As shown in Figure 3A and B, the closure rates of scratch wounds at 24 and 48 h in

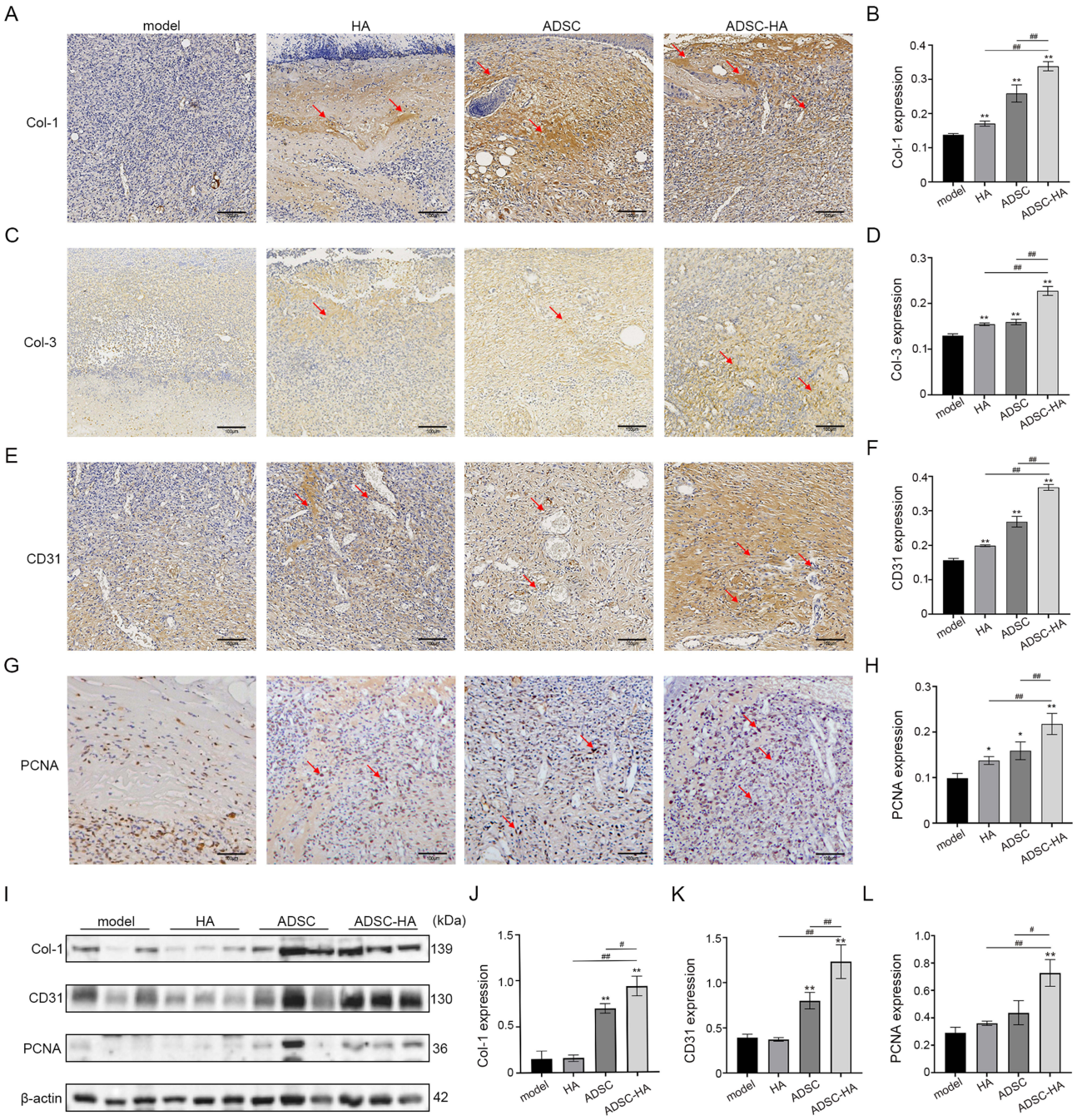

Figure 2 The representative images of immunohistochemical staining and Western blot of mice skin samples. (**A** and **B**) The immunohistochemical staining of Col-1 and the analysis of the positive area with the Image J 1.47 software. (**C** and **D**) The immunohistochemical staining of Col-3 and the analysis of the positive area with the Image J 1.47 software (5X, bar = 200 μm; 10X, bar = 100 μm). (**E** and **F**) The immunohistochemical staining of CD31 and the analysis of the positive area with the Image J 1.47 software (5X, bar = 200 μm; 10X, bar = 100 μm). (**G** and **H**) The immunohistochemical staining of CD31 and the analysis of the positive area with the Image J 1.47 software (10X, bar = 100 μm). (**I–L**) The results of Western blot of Col-1, CD31, and PCNA on day 14 and quantification of protein expression. Data are shown as mean ± SD (n = 3); $^{*}p < 0.05$ vs model, $^{**}p < 0.01$ vs model; $^{\#}p < 0.05$ vs ADSC-HA, $^{\#\#}p < 0.01$ vs ADSC-HA.

ADSC-CM group were significantly higher than that of NC group ($p < 0.05$ or $p < 0.01$ vs NC). As shown in Figure 3C, the results of the CCK-8 assay revealed that ADSC-CM could boost the proliferation of HDFs at concentrations higher than 40% ($p < 0.05$ or $p < 0.01$ vs NC). As shown in Figure 3D–G, the expressions of PCNA, COL1, and COL3 in HDFs were significantly increased after ADSC-CM treatment ($p < 0.05$ or $p < 0.01$ vs NC). Thus, the above results revealed that ADSC-CM could promote wound healing by benefiting the migration, proliferation and collagen production of HDFs.

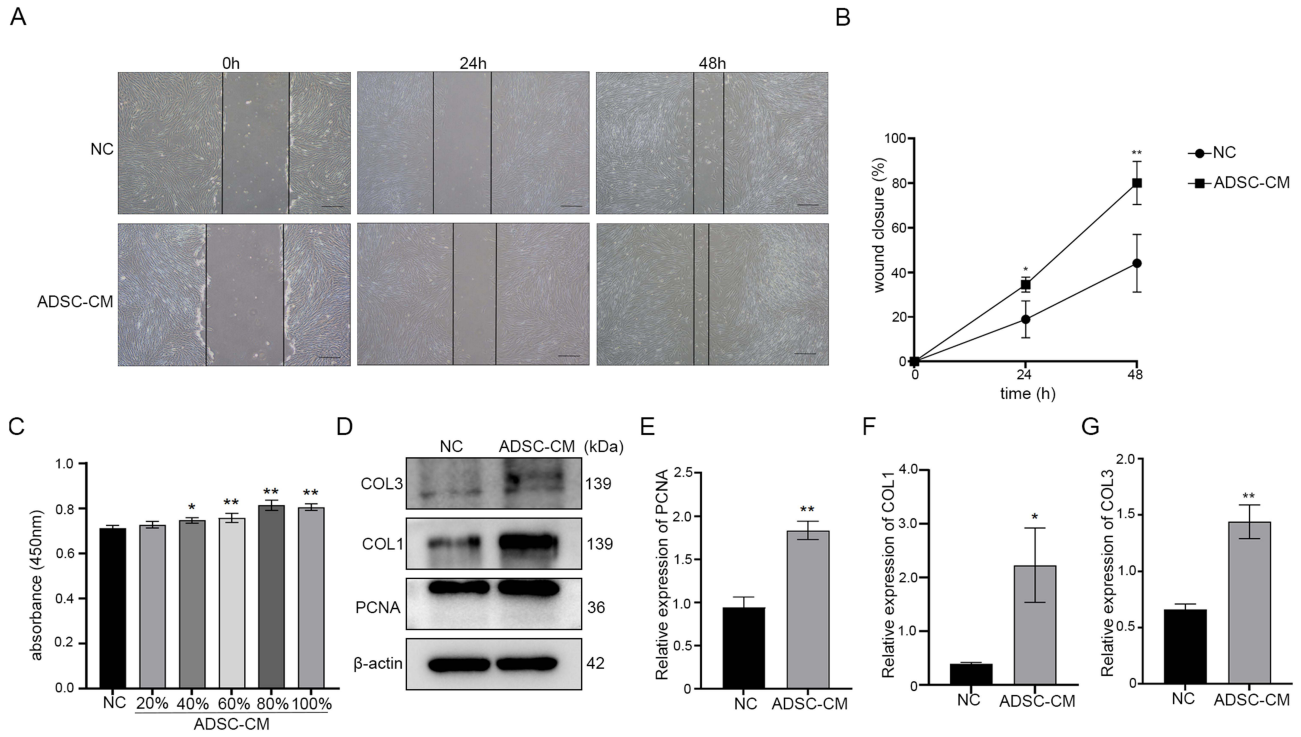

Figure 3 The effects of the conditioned medium of hADSCs (ADSC-CM) on human dermal fibroblasts (HDFs). (**A** and **B**) The representative images of wound healing assay captured at 0, 24, and 48 h (scale bar = 200 μm) and the wound closure rate calculated according to the formula: wound healing rate (%) = $(A_0 - A_t) / A_0 \times 100\%$. A_0 represented the initial wound area and A_t represented the remaining wound area when the measurement was done. (**C**) The results of CCK-8 assay after 48 h treatment of ADSC-CM. (**D–G**) Western blot results of PCNA, COL1, and COL3 after 48 h treatment of ADSC-CM and quantification of protein expression. Data are shown as mean ± SD (n = 3); *$p < 0.05$ vs NC, **$p < 0.01$ vs NC.

ADSC-CM Enhanced the Proliferation, Wound Healing Ability, and Tube Formation of HUVECs in vitro

Wound healing, CCK-8, tube formation, and Western blot assays were conducted to evaluate the proangiogenic effects of ADSC-CM on HUVECs. As shown in Figure 4A and C, the wound healing rates of HUVECs at 24, 48, and 72 h in ADSC-CM group were significantly elevated compared to NC group (all $p < 0.01$ vs NC). As shown in Figure 4B, the results of CCK-8 assay revealed that HUVECs treated with ADSC-CM of each concentration displayed enhanced proliferation (all $p < 0.01$ vs NC). As shown in Figure 4D, ADSC-CM promoted tube formation of HUVECs in terms of generating more branching points and longer tubes at 24, 48, and 72 h ($p < 0.05$ or $p < 0.01$ vs NC). In Figure 4G and H, the Western blot results showed that ADSC-CM upregulated the expression of PCNA in HUVECs compared to the NC group ($p < 0.05$ vs NC). The above findings suggested that ADSC-CM could effectively improve angiogenesis in vitro.

ADSC-CM Improved the Biological Functions of HDFs and HUVECs Under Hypoxic Conditions

Wound healing assay and Western blot were conducted to further explore the effects of ADSC-CM on HDFs and HUVECs under hypoxic conditions. As shown in Figure 5A–D, the wound healing rates of HDFs and HUVECs at 24 h and 48 h in the Hypoxia group were significantly decreased compared to that in the NC group (both $p < 0.01$ vs NC). However, the closure rates of scratch wounds at 24 and 48 h in the Hypoxia + ADSC-CM group were significantly higher than that in the Hypoxia group (all $p < 0.01$ vs Hypoxia).

As shown in Figure 5E–J, the application of $CoCl_2$ elevated the expressions of HIF-1α in the Hypoxic groups of HDFs and HUVECs ($p < 0.05$ or $p < 0.01$ vs NC). In the Hypoxia + ADSC-CM groups of HDFs and HUVECs, the levels of HIF-1α were significantly lower than those in the Hypoxia group ($p < 0.05$ or $p < 0.01$ vs Hypoxia). As shown in

Figure 5E, H, I and L, the expressions of PCNA in HDFs and HUVECs were decreased under hypoxic conditions ($p < 0.05$ or $p < 0.01$ vs NC). The Hypoxia + ADSC-CM group presented higher level of PCNA than the Hypoxia group (both $p < 0.05$ vs Hypoxia), indicating restored proliferative ability of HDFs and HUVECs. As shown in Figure 5E and G, the expression of COL1 was decreased in hypoxic HDFs ($p < 0.01$ vs NC) and was elevated in the Hypoxia + CM group ($p < 0.01$ vs Hypoxia). As shown in Figure 5I and K, CD31 in HUVECs was decreased in the Hypoxia group ($p < 0.05$ vs NC) and was increased in the Hypoxia + CM group ($p < 0.05$ vs Hypoxia). Thus, the above results revealed that hADSCs reversed the adverse effects of hypoxia on HDFs and HUVECs and promoted their biological functions in paracrine way.

Lipid Metabolism and PPARβ/δ Pathway May Mediate the Pressure Ulcer Healing Effect of hADSCs-HA Gel

To elucidate the mechanism of hADSCs-HA gel promoting wound healing of pressure ulcers in mice, a proteomic analysis was conducted. As shown in Figure 6A, a total of 3896 proteins were shared by model, HA, and ADSC-HA groups, which covered 93.54% of the total number of detected proteins. At the same time, there existed 11, 1, and 15 proteins unique to the model, HA, and ADSC-HA group, respectively. The heat map in Figure 5B revealed the enrichment of differentially expressed proteins (DEPs) in the three groups. A significant enrichment of proteins related to lipid metabolism such as Fatty acid-binding protein (P04117), Platelet glycoprotein 4 (Q3U6Y9), Long-chain-fatty-acid-CoA ligase (D3Z041), and Long-chain-fatty-acid-CoA ligase (Q99PU5) was detected in the ADSC-HA and HA group compared to the model group ($p < 0.05$ or $p < 0.01$ vs model). Besides, the expression of Acyl-CoA dehydrogenase family member 11 (A0A087WSI8) was also enriched in the ADSC-HA group compared to the model group ($p < 0.05$ vs model). These findings indicated that hADSCs-HA gel had the potential of facilitating lipid metabolism during the process of wound healing.

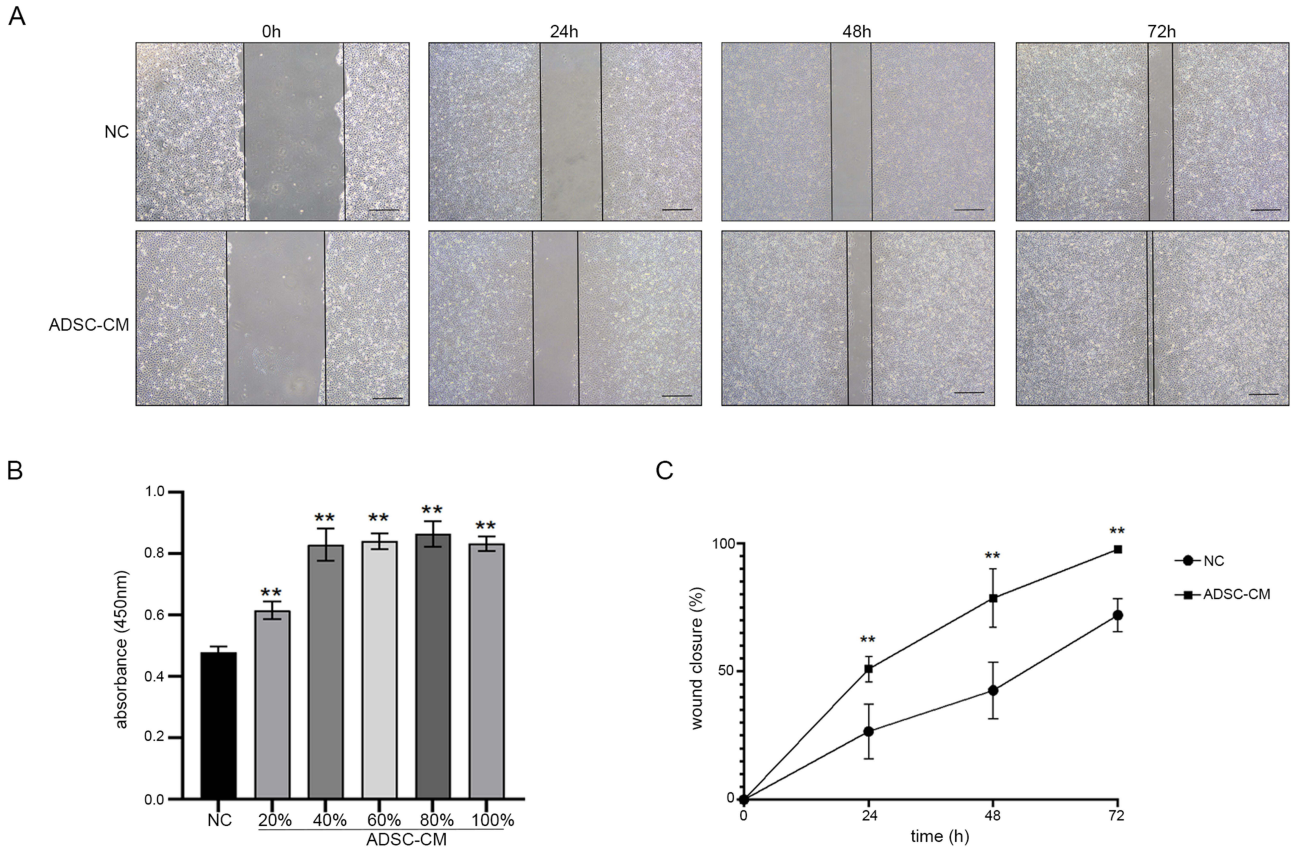

Figure 4 Continued.

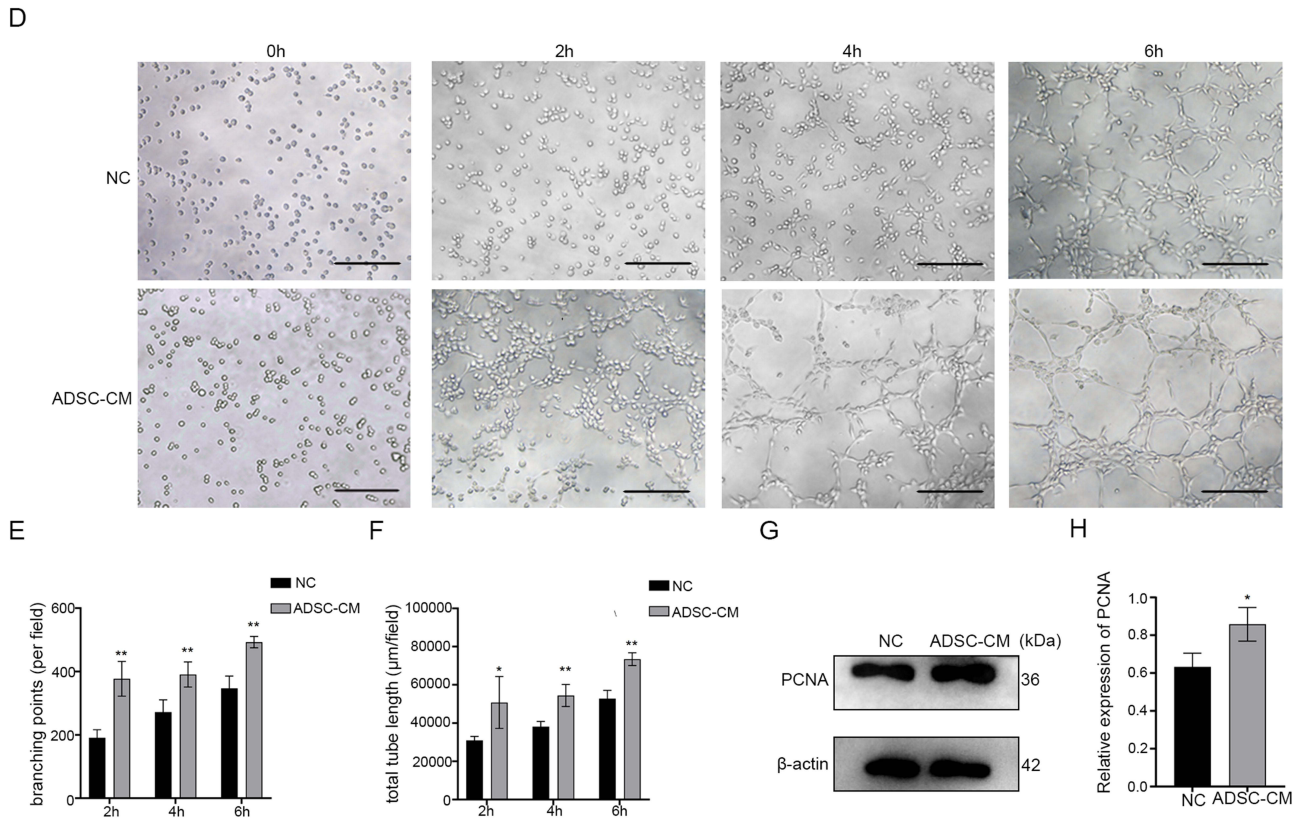

Figure 4 The effects of ADSC-CM on human umbilical vein endothelial cells (HUVECs). (**A** and **C**) The representative images of wound healing assay captured at 0, 24, 48, and 72 h (scale bar = 200 μm) and the wound closure rate calculated according to the formula: wound healing rate (%) = $(A_0 - A_t) / A_0 \times 100\%$. A_0 represented the initial wound area and A_t represented the remaining wound area when the measurement was done. (**B**) The results of CCK-8 assay after 48 h treatment of ADSC-CM. (**D–F**) The results of tube formation assay after 2, 4, and 6 h treatment of ADSC-CM (scale bar = 200 μm) and quantification of branching points and tube length. (**G** and **H**) The results of Western blot of PCNA after 48 h treatment of ADSC-CM and quantification of protein expression. Data are shown as mean ± SD (n = 3); *$p < 0.05$ vs NC; **$p < 0.01$ vs NC.

Next, a quantitative volcano plot was used to reveal the DEPs between the ADSC-HA group and the model group. As shown in Figure 6C, there were 135 up-regulated and 120 down-regulated DEPs detected in the model group compared to the ADSC-HA group. Among them, lipid metabolism-related proteins such as Platelet glycoprotein 4 (Q3U6Y9), Long-chain-fatty-acid-CoA ligase (D3Z041) and Fatty acid-binding protein (P04117) were down-regulated in the model group and this further indicated that the hADSCs-HA gel promoted the healing of pressure ulcer by stimulating lipid utilization.

GO and KEGG enrichment analyses were used to assess all DEPs detected in the model and ADSC-HA group. As shown in Figure 6D, the string graph of GO analysis showed that the DEPs were associated with lipid metabolism functions such as "fatty acid transport", "long-chain fatty acid transport", and 'lipid import into cells'. As shown in Figure 6E, the results of KEGG analysis showed that 16 pathways were significantly enriched in the ADSC-HA group compared with the model group. Among them, there were several fat utilization-related pathways, such as PPARβ/δ signaling pathway, adipocytokine signaling pathway, and fatty acid degradation pathway, suggesting that hADSCs-HA gel may participate in lipid metabolism. It was noteworthy that PPARβ/δ pathway was one of the most significantly enriched KEGG terms ($p < 0.001$ vs model). Figure 6F showed the significant pathways that were notably enriched in the HA group relative to the model group, with a particular focus on the PPARβ/δ signaling pathway. ($p < 0.05$ vs model). We speculated that PPARβ/δ pathway may mediate the effects of hADSC-HA gel on promoting lipid metabolism and wound healing.

PPARβ/δ Pathway-Dependent Mechanism of ADSC-CM on HDFs and HUVECs

To explore the mechanism of PPARβ/δ pathway mediating the pressure ulcer healing effect of hADSCs-HA gel, we further investigated the regulative actions of ADSC-CM at protein levels. GSK3787, which is a selective and irreversible

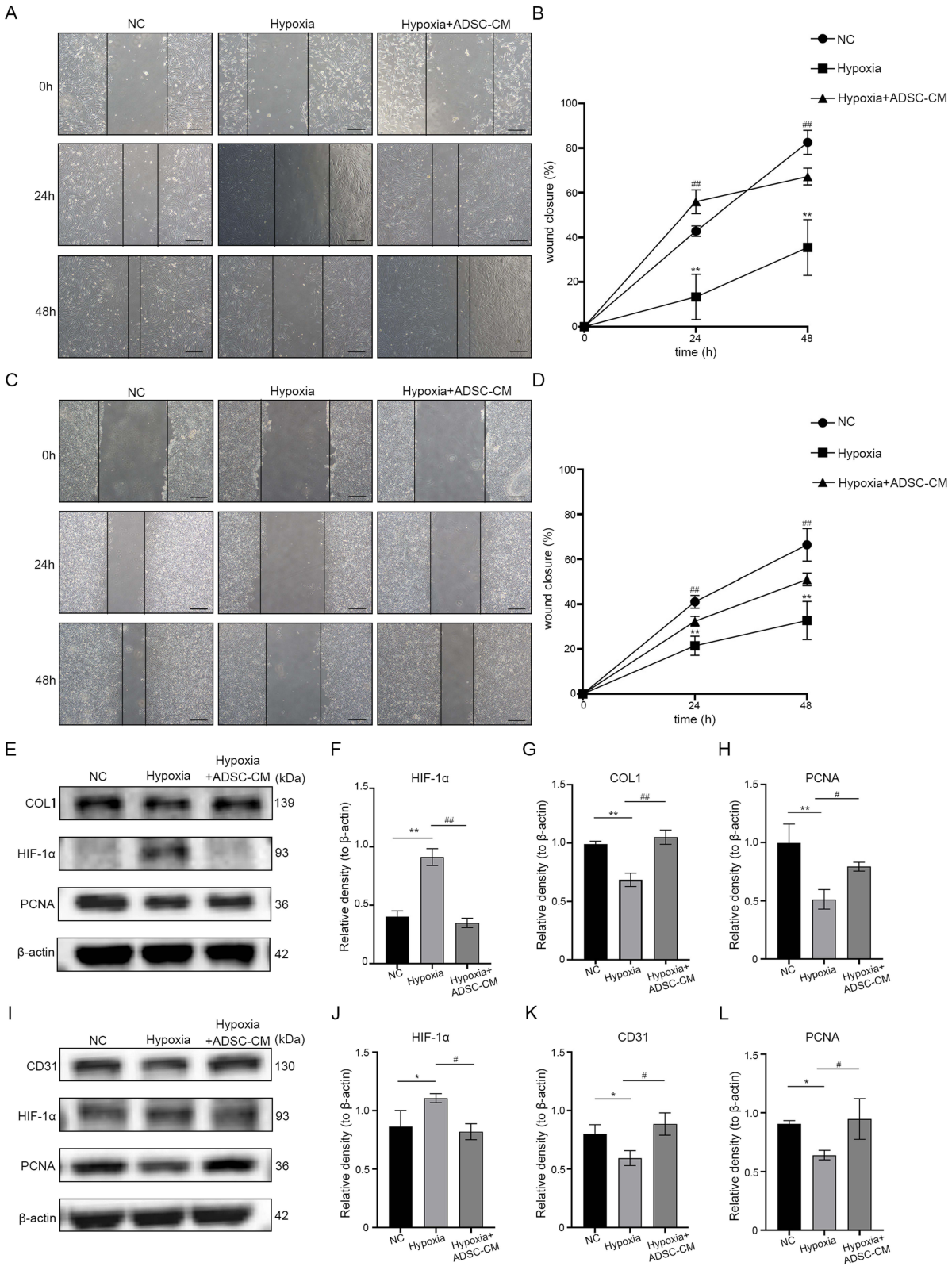

Figure 5 The effects of ADSC-CM on HDFs and HUVECs under hypoxic conditions. (**A–D**) The representative images of wound healing assay captured at 0, 24, and 48 h (scale bar = 200 μm) and the wound closure rate calculated according to the formula: wound healing rate (%) = $(A_0 - A_t) / A_0 \times 100\%$. A_0 represented the initial wound area and A_t represented the remaining wound area when the measurement was done. (**E–H**) Western blot results of COL1, HIF-1α, and PCNA in HDFs after 48 h treatment and quantification of protein expression. (**I–L**) Western blot results of CD31, HIF-1α, and PCNA in HUVECs after 48 h treatment and quantification of protein expression. Data are shown as mean ± SD (n = 3); $^{*}p < 0.05$ vs NC, $^{**}p < 0.01$ vs NC; ns $p \geq 0.05$ vs Hypoxia, $^{\#}p < 0.05$ vs Hypoxia, $^{\#\#}p < 0.01$ vs Hypoxia.

https://doi.org/10.2147/DDDT.S474628 DovePress

inhibitor of PPARβ/δ, was used to verify the PPARβ/δ mechanism. HDFs and HUVECs were seeded into 10 cm plates and divided into 4 groups respectively: NC group, GSK3787 group, ADSC-CM group and ADSC-CM + GSK38787 group. The NC group was treated with HDF-CM or HUVEC-CM. The GSK3787 group was treated with GSK3787 at the

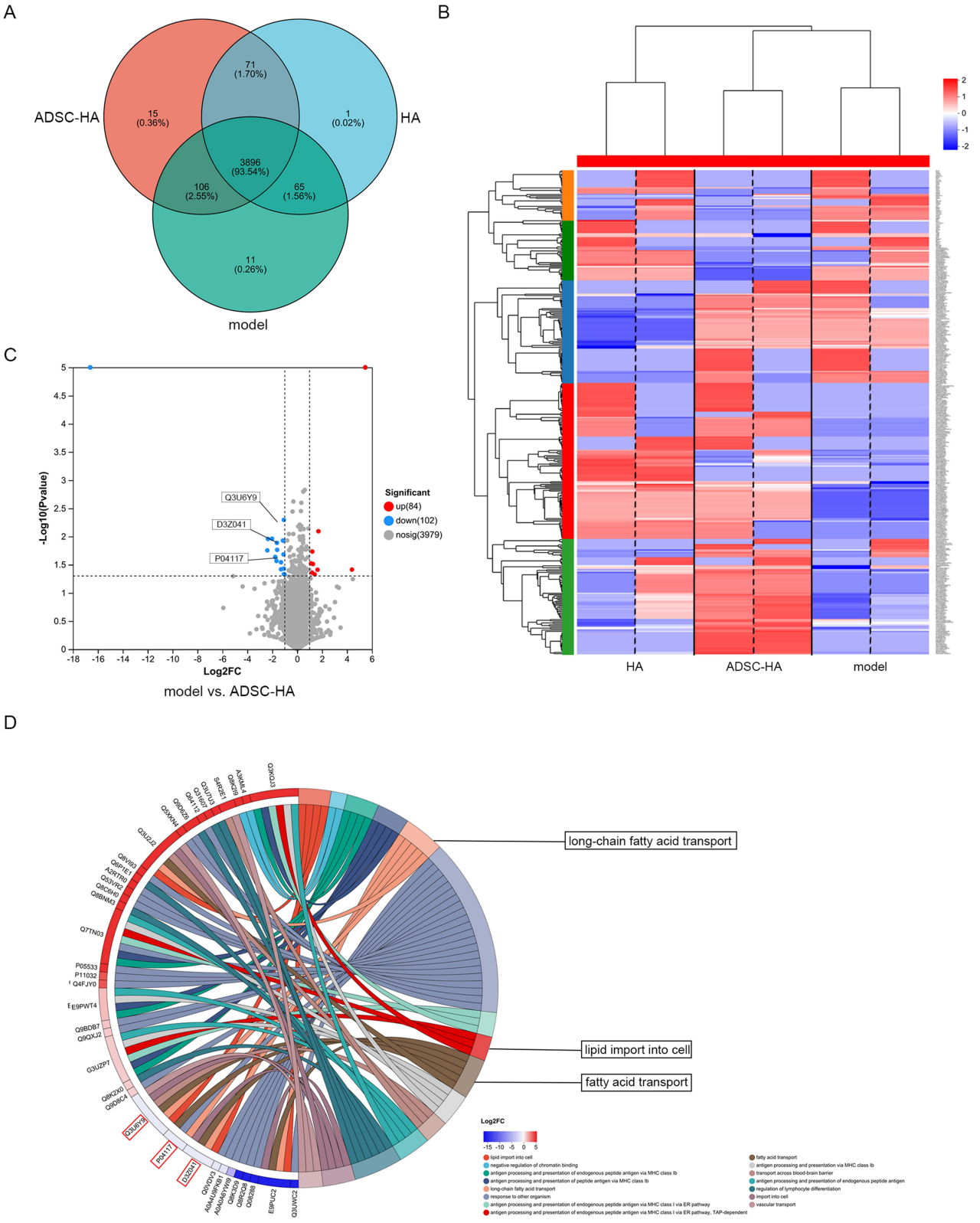

Figure 6 Continued.

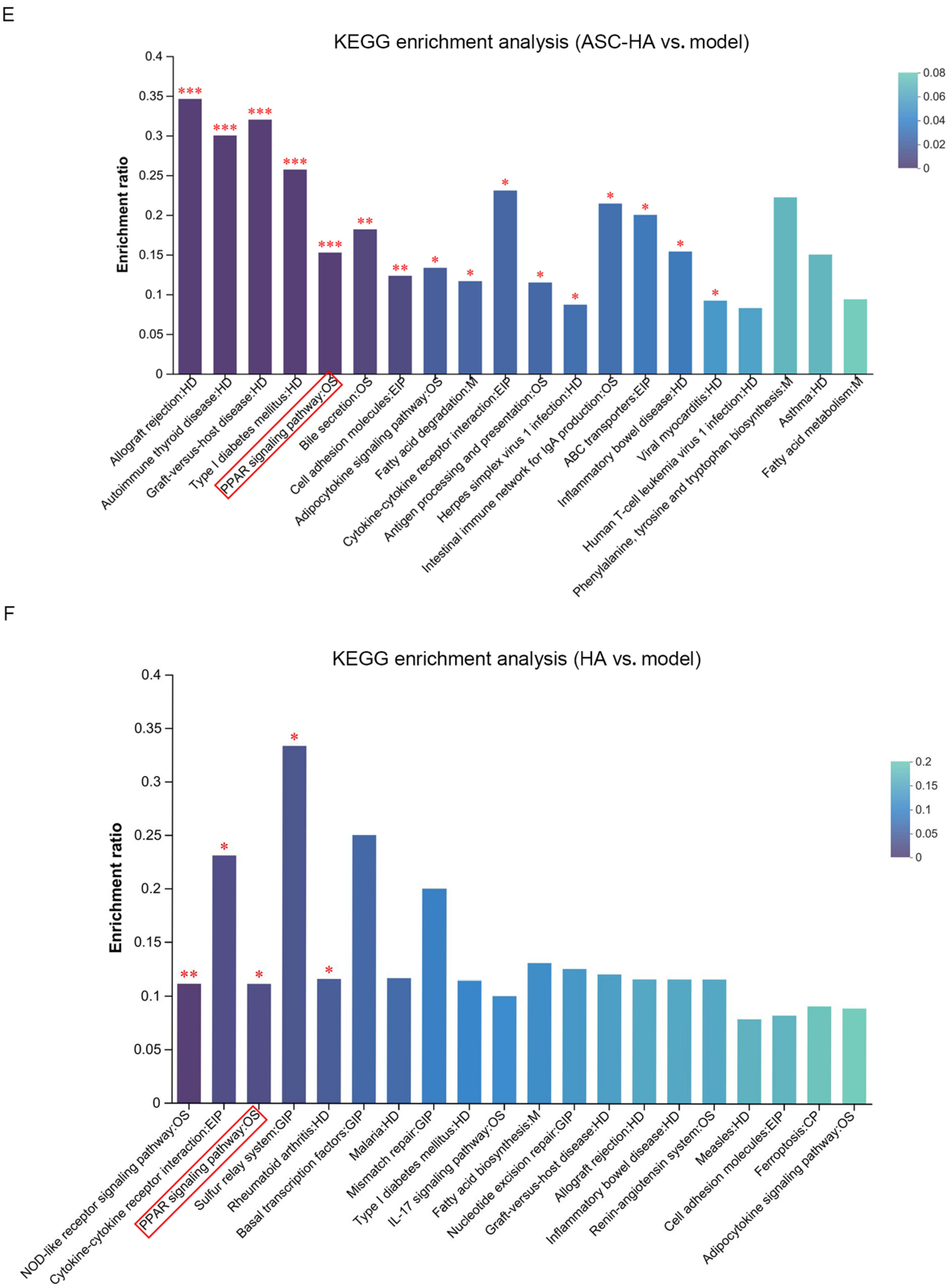

Figure 6 The proteomic analysis of dorsal skin wounds in a mouse pressure ulcer model. (**A**) Venn diagram showing the number of common and unique proteins identified in the model, HA, and ADSC-HA groups. (**B**) The heat map presenting the results of the clustering analysis of the model, HA, and ADSC-HA groups. (**C**) The volcano plot revealing differentially expressed proteins (DEPs) between the ADSC-HA group and the model group. (**D**) The string graph showing the DEPs between the ADSC-HA group and the model group and their corresponding GO terms. The red squares highlighted the typical DEPs related to lipid metabolism. (**E**) KEGG analysis showing the typical pathways where the DEPs between the ADSC-HA group and the model group mainly enriched. The red square highlighted PPARβ/δ pathway which we concentrated on. (**F**) KEGG analysis showing the typical pathways where the DEPs between the HA group and the model group mainly enriched. *$p < 0.05$ vs model; **$p < 0.01$ vs model.

concentration of 1 nM. The ADSC-CM group was treated with ADSC-CM and the ADSC-CM + GSK3787 group was treated with ADSC-CM supplemented with 1 nM GSK3787. After 48 h intervention, total proteins of each group were extracted for Western blot analysis.

As shown in Figure 7A–F, ADSC-CM significantly increased the expressions of COL1 and PCNA in HDFs, which was in parallel with the results shown in Figure 3D (each $p < 0.01$ vs NC). Besides, the expressions of PPARβ/δ pathway proteins (PPARβ/δ and ANGPTL4) were significantly up-regulated after ADSC-CM treatment in HDFs (each $p < 0.05$ or $p < 0.01$ vs NC). As revealed in Figure 7B, G, H, and I, ADSC-CM significantly increased the expressions of PPARβ/δ, ANGPTL4, and CD31 in HUVECs (each $p < 0.05$ or $p < 0.01$ vs NC). For verification, an antagonist of PPARβ/δ (GSK3787) was used to counteract the actions of ADSC-CM. As shown in Figure 7, combined treatment of ADSC-CM

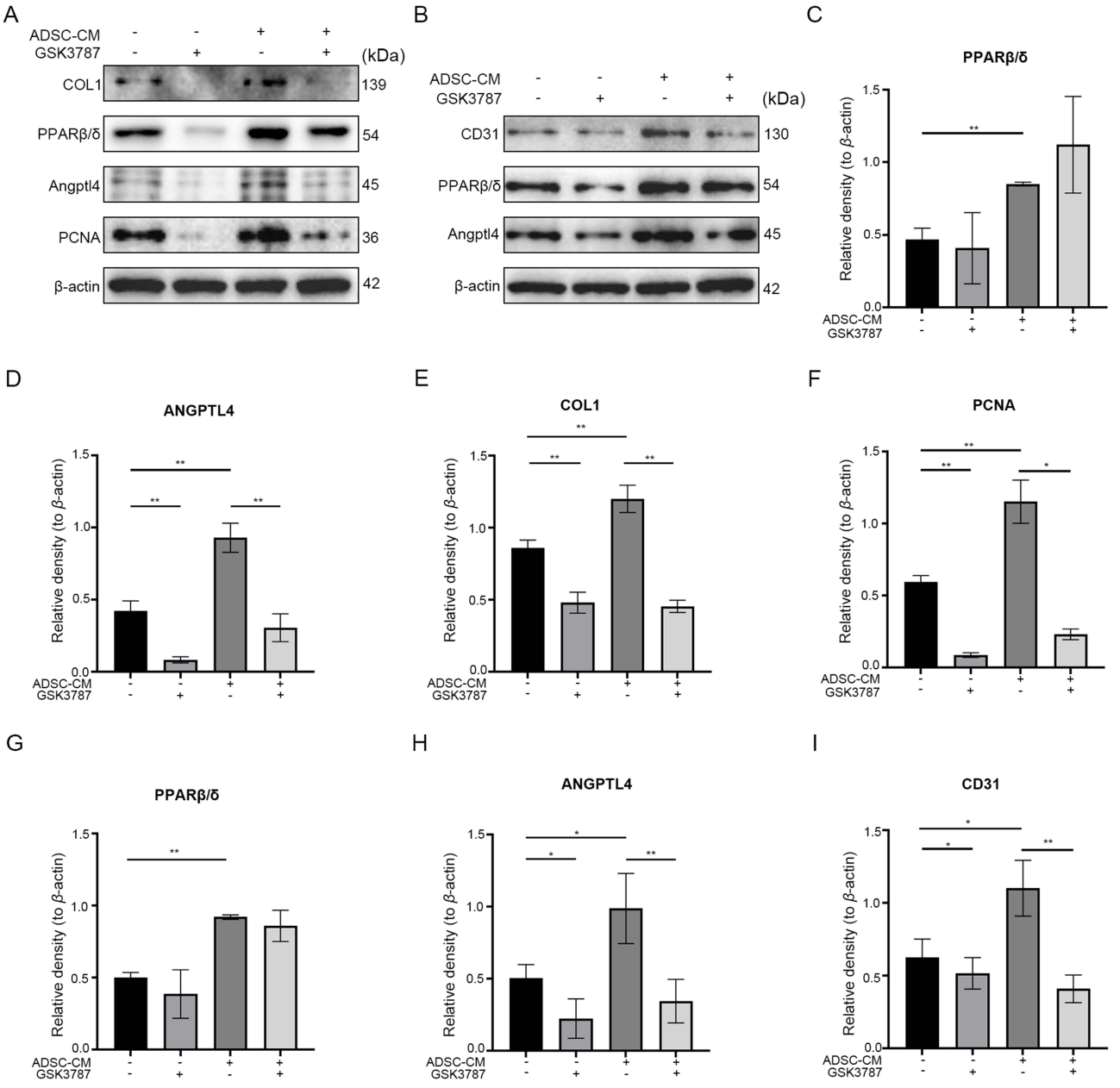

Figure 7 Verification of the regulative effects of hADSCs-HA gel on PPARβ/δ pathway by Western blot (WB). (**A**) Representative WB bands of PPARβ/δ, ANGPTL4, COL1, PCNA in HDFs following 48 h treatment of ADSC-CM or 1 nM GSK3787. (**B**) Representative WB bands of PPARβ/δ, ANGPTL4, CD31 in HUVECs following 48 h treatment of ADSC-CM or 1 nM GSK3787. (**C–F**) Expressions of PPARβ/δ pathway (PPARβ/δ, ANGPTL4), collagen synthesis (COL1) and proliferation (PCNA)-related proteins in HDFs after GSK3787 intervention. (**G–I**) Expressions of PPARβ/δ pathway (PPARβ/δ, ANGPTL4) and angiogenesis (CD31)-related proteins in HUVECs after GSK3787 intervention. Data are shown as mean ± SD (n = 3); *$p < 0.05$; **$p < 0.01$.

and GSK3787 not only reversed the regulative actions of ADSC-CM on collagen synthesis (COL1) and proliferation (PCNA)-related proteins in HDFs, but also angiogenesis (CD31)-related protein in HUVECs (each $p < 0.05$ or $p < 0.01$ vs ADSC-CM). Moreover, GSK3787 counteracted the activated PPARβ/δ pathway regulation of ADSC-CM in both HDFs and HUVECs ($p < 0.01$ vs ADSC-CM). The above results indicated that ADSC-CM improved the collagen synthesis and proliferation of HDFs and the angiogenesis of HUVECs through the activation of PPARβ/δ pathway.

Discussion

Utilizing mice pressure ulcer model, our study achieved a profound insight into the therapeutic value and underlying molecular mechanism of hADSCs-HA gel in treating pressure ulcers. The animal experiment demonstrated that hADSCs-HA gel accelerated pressure ulcers healing, which performed better than applying hADSCs or HA respectively. In terms of histopathology, hADSCs-HA gel elevated the expression of Col-1, Col-3, PCNA, and CD31 in skin, which verified its role in promoting collagen secretion, skin proliferation, and angiogenesis. In previous studies, several kinds of MSCs have been used to treat pressure ulcers in the form of cell solution for injection. Bukowska et al demonstrated that by injecting freshly cultured and cryopreserved hASCs, pressure wound repair accelerated in both young male and female immunocompetent mice.[36] In another study, Yoon et al proved that subcutaneous injection of fibroblasts differentiated from mesenchymal stem cells derived from human embryonic stem cell improved the healing of pressure ulcers by suppressing inflammatory genes and stimulating angiogenesis.[69] In our study, we optimized the delivery of hADSCs by topical application of hADSCs-HA gel and minimized the risk of secondary trauma and infection. At the same time, the cellular data showed that ADSC-CM improved the functions of HDFs and HUVECs under both normal and hypoxic conditions, indicating that hADSCs-HA gel promoted wound healing through paracrine pathway. In previous studies, Dong et al found that with the delivery of HA, spreading, proliferation, and secretion of stem cells were facilitated.[70] Jiao et al found that HA prolonged the retention of stem cells and also potentiated their paracrine function in treating ovarian aging.[71] Our study also substantiated the role of HA as a promising carrier to apply hADSCs on pressure wounds which allowed hADSCs to maintain paracrine function. In a word, the innovation of our study lies in: 1) topical application of hADSCs-HA gel instead of invasive therapy; 2) demonstration of the protective effects of hADSCs on HDFs and HUVECs under hypoxic conditions; 3) clarification of PPARβ/δ paracrine mechanism of hADSCs on wound healing.Widely distributed in many systems of human body, adipocytes have received increasing recognition as important contributors to tissue homeostasis and repair. Distinct from those in subcutaneous white adipose tissue in aspects of anatomy, structure, and function, adipocytes residing in dermis have been proved to play a crucial role in hair growth, wound healing, and thermoregulation in recent work.[72] As reported by Shook et al, when skin wounds occur, several kinds of fatty acid are released by dermal adipocytes such as palmitoleic acid and oleic acid leading to the activation of macrophages in the wound area.[73] In addition, adipocytes also participate in endocrine signaling by secreting a wide range of "adipokines", among which adiponectin and leptin have been reported as active contributors in wound healing by stimulating re-epithelization and re-vascularization.[74–78] Also, the process of adipogenesis is proved to actively engaged in wound healing by recruiting fibroblasts and orchestrating with angiogenesis.[79,80] Existing studies have demonstrated that with the transplantation of adipose tissue or hADSCs, adipogenesis of injured skin can be strengthened.[35,81,82] However, the underlying mechanism has not yet been fully clarified. PPAR pathway, a core mediator of adipogenesis and lipid metabolism, is also potentially associated with tissue regeneration.[83–85] According to the results of our proteomic analysis, PPAR pathway was enriched by the detected DEPs, implicating its latent value in regulating the therapeutic effects of hADSCs-HA gel.

PPARs are nuclear hormone receptors and belong to a subfamily of transcription nuclear factors.[86] There are three isotypes of PPARs known as PPARα, PPARβ/δ and PPARγ. PPARα is highly expressed in the tissues involved with β-oxidation of fatty acid such as liver, skeletal muscle, and heart, and plays a vital role in starvation and feeding response.[87,88] It has also been proved to have anti-inflammatory and neuro-protective effects.[89–91] PPARγ is the most studied one among the three isoforms. Mainly distributed in adipose tissue, PPARγ is an important modulator of adipogenesis, adipocyte differentiation, and lipid storage, and also acts as the regulator of insulin sensitivity.[92–94] Among the three isoforms, the functions of PPARβ/δ remain least understood. Abundantly distributed in brain, adipose tissue, and skin, PPARβ/δ acts as the bridge between metabolism and regeneration, and participates in important

processes involved in regeneration including proliferation, differentiation, migration, angiogenesis, and so on.[95–97] However, the role of PPARβ/δ in healing of skin wounds has received limited consideration. Previous studies found that activation of PPARβ/δ in wounds maintained survival of keratinocytes and promoted their migration through PI3K/PIP3 pathway, leading to accelerated re-epithelialization.[98–100] PPARβ/δ also promotes proliferation of endothelial cells (ECs) and endothelial progenitor cells by enhancing their glycolysis and energy use.[101,102] However, the mechanism of this instability is still unclear. As to skin fibroblasts, there have been little clues about how they response to regulation of PPARβ/δ.

Our studied shed some light on how PPARβ/δ impact on HDFs and HUVECs, and demonstrated how ADSC-CM modulated this process for the first time. After binding with RXR, PPARβ/δ forms a complex to activate transcription of various target genes, among which ANGPTL4 is one of the most important downstream genes of PPARβ/δ. In addition to weakening cellular tight junctions, ANGPTL4 could induce the production of nitric oxide (NO) in wound epithelia through integrin/JAK/STAT3-mediated up-regulation of inducible nitric oxide synthase (iNOS) expression. Such novel mechanism gives rise to angiogenesis in wounds and is named as keratinocyte-to-endothelial cell communication.[103] ANGPTL4 also modulates integrity of matrix proteins to facilitate cell migration and maintain homeostasis of microenviroment.[104,105] However, most of previous studies examined the paracrine function of ANGPTL4, while its potential cell-autonomous roles were neglected.[106] In our study, ADSC-CM evoked up-regulation of both PPARβ/δ and ANGPTL4 in HDFs and HUVECs. In contrast, when PPARβ/δ pathway was blocked by GSK3787, the expression of ANGPTL4 was suppressed and such trend could be reversed by application of ADSC-CM. These findings indicated that ADSC-CM stimulated PPARβ/δ pathway as an upstream activator. At the same time, the level of PCNA, an important biomarker of cell proliferation,[107] was elevated by ADSC-CM and declined by inhibition of PPARβ/δ in both HDFs and HUVECs. It followed that PCNA was also a potential target gene of PPARβ/δ and paracrine functions of hADSCs influenced the proliferation phase of wound healing positively by enhancing activity of PPARβ/δ axis. At the end of inflammatory phase and beginning of proliferation phase of wound, activated fibroblasts produce several matrix metalloproteinases (MMPs) that penetrate and break down fibrin clot, replacing it with ECM components. Among them, COL1 plays an important role in refilling the defect and restoring ECM.[108] On the other hand, CD31, also known as platelet endothelial cell adhesion molecule-1, is widely involved in proangiogenic events such as migration, adhesion, and proliferation of ECs during wound healing. In our study, COL1 in fibroblasts and CD31 in HUVCEs showed the same trends of expression with ANGPTL4 and PCNA. Based on this, we could conclude that PPARβ/δ promoted regeneration of vessels and ECM in wound sites, and mediated the paracrine effects of hADSCs on the restoration of wound micro-environments. It is noteworthy that in a recent study, a kind of Lignin/Puerarin Nanoparticle-Incorporated Hydrogel was developed to treat mice hind-limb ischemia model and was found to upregulate PPARβ/δ by stimulating autophagy.[109] Interestingly, another latest article showed that exosomes of hADSCs promoted diabetic wound repair by stimulating autophagy of skin cells.[110] In light of our experimental findings, the paracrine activation of PPARβ/δ by hADSCs may be closely related to autophagy, which still needs further verification. In previous studies, the activation of PPARβ/δ suppressed inflammation and promoted angiogenesis by regulating macrophage phenotype and IL-1 expression.[111,112] Besides, the activation of PPARβ/δ also induced fibroblasts to produce GPx1 and catalase, which can scavenge excess H_2O_2 in diabetic wound beds.[113] These findings imply that the promotion of PPARβ/δ by hADSCs may involve upstream and downstream regulatory mechanism, which is valuable for further exploration.

The healing of pressure ulcers is a complicated and dynamic process under sophisticated control of oxygen concentration at the wound site, which involves the interaction of multiple mechanisms. In our study, both HDFs and HUVECs under hypoxic conditions showed high expression of HIF-1α, but the wound healing capacity and markers of proliferation (PCNA), angiogenesis (CD31), and collagen synthesis (COL1) were reduced. The activation of HIf-1α is the core pathway of hypoxic adaptation, stimulating inflammatory responses, angiogenesis, and metabolic reprogramming.[114] However, as a survival factor during the first hours of hypoxia, the overactivation of HIF-1α also acts as a death-promoting factor when the hypoxia is prolonged.[115] Besides, hypoxic microenvironment also directly induces mitochondrial fragmentation and ubiquitination, inhibiting oxidative phosphorylation and leading to cell apoptosis.[116,117] Additionally, by activating JNK and DDIT3, hypoxia inhibits adaptive unfolded protein response (UPR), thus aggravating endoplasmic reticulum (ER) stress and cell apoptosis, but this process is independent of HIF-

1α.[118] Several previous studies have confirmed that MSCs play a positive role in the regulation of cell biological functions under hypoxic conditions. Wilai Kosol et al found that the secretome of MSCs reversed the inhibitory effects of hypoxia on keratinocyte proliferation and migration, contributing to the acceleration of wound healing.[119] The study by Chunling Liao et al confirmed that conditioned medium of MSC protected renal tubular epithelial cells in hypoxia by downregulating HIF-1α.[120] In our study, ADSC-CM decreased the expression of HIF-1α and promoted the biological functions of HDFs and HUVECs under hypoxic conditions. Previous studies proved that the activation of PPARβ/δ boosted fatty acid oxidation and improved mitochondrial function via the AMPK-p53-GDF15 pathway.[121] Such processes lowered ROS production, ER stress, and mitochondrial damage induced by hypoxia, thus protecting cells against hypoxic damage.[122] Furthermore, it was also been demonstrated that PPARβ/δ and HIF-1α achieved synergistic transcriptional regulation of the co-target gene ANGPTL4 by altering the metachromatic plasma conformation, which stimulated angiogenesis.[123] In parallel with these, in vitro data of our study proved that hADSCs stimulated PPARβ/δ and ANGPTL4 in both HDFs and HUVECs, which may also act as the approach to protect cells under hypoxic conditions. However, the underlying mechanism still needs further exploration.

Another implication of our study is the optimization of stem cell delivery in wound treatment. By innovatively encapsulating hADSCs in HA, we demonstrated that the therapeutic efficacy of such combination was greater than that of HA or hADSCs alone. Compared with commercial collagen gel, hADSCs-HA gel significantly accelerated the healing of pressure ulcers by promoting collagen regeneration, angiogenesis, and skin cell proliferation. Our study also showed that hADSCs modulated lipid metabolism and promoted healing in paracrine way, which distinguished hADSCs-HA gel from other wound-healing materials. Another advantage of hADSCs-HA gel is the superior biocompatibility of HA compared with other scaffold materials, improving the stability and activity of stem cells in wound sites. Besides, the topical application of hADSCs-HA gel also enhances its usability, safety and potential for clinical translation. In recent years, topical application of hydrogel-based stem cell therapy has gained increasing attention in the treatment of various chronic wounds. In previous studies, gelatin-based hydrogel (GBH) wound dressing combined with ADSCs improved wound healing in both mice and porcine.[124] A photo-active gelatin (Az-Gel) modified stem cell seeded bilayer PVA hydrogel dressings with silver nanoparticles loaded poly (lactic-co-glycolic acid) (PLGA) electrospinning films (Ag-PLGA) presented great biocompatibility and anti-bacterial activity. Such hydrogel allowed the bioactive factors secreted by ADSCs to penetrate and promoted cell growth and wound healing.[125] In addition, an enzyme-crosslinked gelatin hydrogel containing ADSC spheroid was successfully prepared. It significantly boosted the regeneration of epidermis and improved wound architecture.[126] Besides, in a clinical study, hydrogel-based allogeneic ADSCs sheets was used to treat diabetic ulcers and 82% of the patients in treatment group achieved complete wound closure within 12 weeks.[127] Compared with above-mentioned hydrogels, hADSCs-HA exihibits multiple advantages such as simple preparation, convenient application, and less triggering of immune responses. Accordingly, we believe that hADSCs-HA gel has broad prospects in clinical application. In addition to pressure ulcers, hADSCs-HA gel also possesses potentials in treating diabetic ulcers, burn wounds, and radioactive damages. However, clinical translation of hADSCs-HA gel still faces some obstacles. The limitations of our study mainly include the following aspects: (1) hADSCs are varied due to differences in donor age, sex, body mass index, clinical status, and cell sampling location, therefore the quality control of hADSCs-HA gel before clinical application is still an urgent problem; (2) The biocompatibility of hADSCs-HA gel still needs further research; (3) In our study, hADSCs-HA gel was prepared immediately before use. However, the storage conditions of gel still need to be explored to facilitate clinical application.

Conclusion

This study demonstrated the promotive efficacy of hADSCs-HA gel on mice pressure ulcers and clarified the PPARβ/δ-related paracrine mechanism underlying the effects of ADSC-CM on HDFs and HUVECs. In vivo, hADSCs-HA gel accelerated the healing of pressures ulcers during the proliferative phase by promoting collagen synthesis and vascularization. In vitro, hADSCs improved the biological properties of HDFs and HUVECs in a paracrine manner by facilitating their proliferation, boosting their migration and elevating their expression of proteins related with wound healing. ADSC-CM was also observed to promote the functions of HDFs and HUVECs under hypoxic conditions. With the aid of proteomics analysis, we also verified that such paracrine functions of ADSC-CM were achieved through the activation of

PPARβ/δ pathway. Therefore, hADSCs-HA gel is a promising therapeutic candidate for treating pressure ulcers topically. Overall, this work contributed new understanding about the ability of MSCs to wound restoration, and this has significance in the application of stem cells in clinical background.

Data Sharing Statement

The datasets used and analysed during the current study are available from the corresponding author on reasonable request.

Ethics Approval and Consent to Participate

All animal experimental procedures were performed according to the guidelines for the Care and Use of Laboratory Animals of the National Institutes of Health and were approved by the Medical Norms and Ethics Committee of Zhejiang Chinese Medical University (grant number: 20210705-12).

Acknowledgments

The graphical abstract was completed by Figdraw (ID: YUWII039bb).

Author Contributions

All authors made a significant contribution to the work reported, whether that is in the conception, study design, execution, acquisition of data, analysis and interpretation, or in all these areas; took part in drafting, revising or critically reviewing the article; gave final approval of the version to be published; have agreed on the journal to which the article has been submitted; and agree to be accountable for all aspects of the work.

Funding

This work was supported by Zhejiang Provincial Natural Science Foundation of China (Grant No. LGF22H150017), Zhejiang Provincial Military Medical Science and Technology Youth Cultivation Program (Grant No. 19QNP045), and Zhejiang Provincial Medical Science and Technology Program (Grant No. 2019315077).

Disclosure

The authors declare no competing interests in this work.

References

1. Stages NF. Pressure ulcer stages revised by the National Pressure Ulcer Advisory Panel. *Ostomy Wound Manage*. 2007;53(3):30–31.
2. Peirce SM, Skalak TC, Rodeheaver GT. Ischemia-reperfusion injury in chronic pressure ulcer formation: a skin model in the rat. *Wound Repair Regen*. 2000;8(1):68–76. doi:10.1046/j.1524-475x.2000.00068.x
3. Mervis JS, Phillips TJ. Pressure ulcers: pathophysiology, epidemiology, risk factors, and presentation. *J Am Acad Dermatol*. 2019;81(4):881–890. doi:10.1016/j.jaad.2018.12.069
4. Guan Y, Niu H, Liu Z, et al. Sustained oxygenation accelerates diabetic wound healing by promoting epithelialization and angiogenesis and decreasing inflammation. *Sci Adv*. 2021;7(35). doi:10.1126/sciadv.abj0153
5. Schreml S, Szeimies RM, Prantl L, Karrer S, Landthaler M, Babilas P. Oxygen in acute and chronic wound healing. *Br J Dermatol*. 2010;163(2):257–268. doi:10.1111/j.1365-2133.2010.09804.x
6. Eaton L, Pamenter ME. What to do with low O(2): redox adaptations in vertebrates native to hypoxic environments. *Comp Biochem Physiol a Mol Integr Physiol*. 2022;271:111259. doi:10.1016/j.cbpa.2022.111259
7. Fuhrmann DC, Brune B. Mitochondrial composition and function under the control of hypoxia. *Redox Biol*. 2017;12:208–215. doi:10.1016/j.redox.2017.02.012
8. Chou R. Pressure ulcer risk assessment and prevention. *Ann Intern Med*. 2013;159(10):718–719. doi:10.7326/0003-4819-159-10-201311190-00017
9. Lyder CH. Pressure ulcer prevention and management. *JAMA*. 2003;289(2):223–226. doi:10.1001/jama.289.2.223
10. Morton LM, Phillips TJ. Wound healing and treating wounds: differential diagnosis and evaluation of chronic wounds. *J Am Acad Dermatol*. 2016;74(4):589–605;quiz605–6. doi:10.1016/j.jaad.2015.08.068
11. Smith ME, Totten A, Hickam DH, et al. Pressure ulcer treatment strategies: a systematic comparative effectiveness review. *Ann Intern Med*. 2013;159(1):39–50. doi:10.7326/0003-4819-159-1-201307020-00007
12. Fox C. Living with a pressure ulcer: a descriptive study of patients' experiences. *Br J Community Nurs*. 2002;7(6 Suppl):22. doi:10.12968/bjcn.2002.7.Sup4.12615

13. Spilsbury K, Nelson A, Cullum N, Iglesias C, Nixon J, Mason S. Pressure ulcers and their treatment and effects on quality of life: hospital inpatient perspectives. *J Adv Nurs*. 2007;57(5):494–504. doi:10.1111/j.1365-2648.2006.04140.x
14. Mondragon N, Zito PM. Pressure Injury. In: *StatPearls*. StatPearls Pub; 2023.
15. Wong JK, Amin K, Dumville JC. Reconstructive surgery for treating pressure ulcers. *Cochrane Database Syst Rev*. 2016;12(12):CD012032. doi:10.1002/14651858.CD012032.pub2
16. VanGilder C, Lachenbruch CA. Air-fluidized therapy: physical properties and clinical uses. *Ann Plast Surg*. 2010;65(3):364–370. doi:10.1097/SAP.0b013e3181cd3d73
17. Harrison-Balestra C, Eaglstein WH, Falabela AF, Kirsner RS. Recombinant human platelet-derived growth factor for refractory nondiabetic ulcers: a retrospective series. *Dermatol Surg*. 2002;28(8):755–759. doi:10.1046/j.1524-4725.2002.02004.x
18. Kuroyanagi Y, Yamada N, Yamashita R, Uchinuma E. Tissue-engineered product: allogeneic cultured dermal substitute composed of spongy collagen with fibroblasts. *Artif Organs*. 2001;25(3):180–186. doi:10.1046/j.1525-1594.2001.025003180.x
19. Sharma V, Kohli N, Moulding D, et al. Design of a novel two-component hybrid dermal scaffold for the treatment of pressure sores. *Macromol Biosci*. 2017;17(11). doi:10.1002/mabi.201700185
20. Zeng N, Chen H, Wu Y, Liu Z. Adipose stem cell-based treatments for wound healing. *Front Cell Dev Biol*. 2021;9:821652. doi:10.3389/fcell.2021.821652
21. Shingyochi Y, Orbay H, Mizuno H. Adipose-derived stem cells for wound repair and regeneration. *Expert Opin Biol Ther*. 2015;15(9):1285–1292. doi:10.1517/14712598.2015.1053867
22. Hassanshahi A, Hassanshahi M, Khabbazi S, et al. Adipose-derived stem cells for wound healing. *J Cell Physiol*. 2019;234(6):7903–7914. doi:10.1002/jcp.27922
23. Lo Sicco C, Reverberi D, Balbi C, et al. Mesenchymal stem cell-derived extracellular vesicles as mediators of anti-inflammatory effects: endorsement of macrophage polarization. *Stem Cells Transl Med*. 2017;6(3):1018–1028. doi:10.1002/sctm.16-0363
24. Ajit A, Kumar TRS, Harikrishnan VS, Anil A, Sabareeswaran A, Krishnan LK. Enriched adipose stem cell secretome as an effective therapeutic strategy for in vivo wound repair and angiogenesis. *3 Biotech*. 2023;13(3):83. doi:10.1007/s13205-023-03496-0
25. Zhang W, Bai X, Zhao B, et al. Cell-free therapy based on adipose tissue stem cell-derived exosomes promotes wound healing via the PI3K/Akt signaling pathway. *Exp Cell Res*. 2018;370(2):333–342. doi:10.1016/j.yexcr.2018.06.035
26. Ren S, Chen J, Duscher D, et al. Microvesicles from human adipose stem cells promote wound healing by optimizing cellular functions via AKT and ERK signaling pathways. *Stem Cell Res Ther*. 2019;10(1):47. doi:10.1186/s13287-019-1152-x
27. Bi H, Li H, Zhang C, et al. Stromal vascular fraction promotes migration of fibroblasts and angiogenesis through regulation of extracellular matrix in the skin wound healing process. *Stem Cell Res Ther*. 2019;10(1):302. doi:10.1186/s13287-019-1415-6
28. Cerqueira MT, Pirraco RP, Santos TC, et al. Human adipose stem cells cell sheet constructs impact epidermal morphogenesis in full-thickness excisional wounds. *Biomacromolecules*. 2013;14(11):3997–4008. doi:10.1021/bm4011062
29. Imai Y, Mori N, Nihashi Y, et al. Therapeutic potential of adipose stem cell-derived conditioned medium on scar contraction model. *Biomedicines*. 2022;10:10. doi:10.3390/biomedicines10102388
30. Liang J, Zhang H, Kong W, et al. Safety analysis in patients with autoimmune disease receiving allogeneic mesenchymal stem cells infusion: a long-term retrospective study. *Stem Cell Res Ther*. 2018;9(1):312. doi:10.1186/s13287-018-1053-4
31. Moon KC, Chung HY, Han SK, Jeong SH, Dhong ES. Possibility of injecting adipose-derived stromal vascular fraction cells to accelerate microcirculation in ischemic diabetic feet: a pilot study. *Int J Stem Cells*. 2019;12(1):107–113. doi:10.15283/ijsc18101
32. Raposio E, Bertozzi N, Bonomini S, et al. Adipose-derived stem cells added to platelet-rich plasma for chronic skin ulcer therapy. *Wounds*. 2016;28(4):126–131.
33. Tarallo M, Fino P, Ribuffo D, et al. Liposuction aspirate fluid adipose-derived stem cell injection and secondary healing in fingertip injury: a pilot study. *Plast Reconstr Surg*. 2018;142(1):136–147. doi:10.1097/PRS.0000000000004506
34. Na YK, Ban JJ, Lee M, Im W, Kim M. Wound healing potential of adipose tissue stem cell extract. *Biochem Biophys Res Commun*. 2017;485(1):30–34. doi:10.1016/j.bbrc.2017.01.103
35. Strong AL, Bowles AC, MacCrimmon CP, et al. Adipose stromal cells repair pressure ulcers in both young and elderly mice: potential role of adipogenesis in skin repair. *Stem Cells Transl Med*. 2015;4(6):632–642. doi:10.5966/sctm.2014-0235
36. Bukowska J, Alarcon Uquillas A, Wu X, et al. Safety and efficacy of human adipose-derived stromal/stem cell therapy in an immunocompetent murine pressure ulcer model. *Stem Cells Dev*. 2020;29(7):440–451. doi:10.1089/scd.2019.0244
37. Fallacara A, Baldini E, Manfredini S, Vertuani S. Hyaluronic acid in the third millennium. *Polymers (Basel)*. 2018;10(7):701. doi:10.3390/polym10070701
38. Graca MFP, Miguel SP, Cabral CSD, Correia IJ. Hyaluronic acid-Based wound dressings: a review. *Carbohydr Polym*. 2020;241:116364. doi:10.1016/j.carbpol.2020.116364
39. Salathia S, Gigliobianco MR, Casadidio C, Di Martino P, Censi R. Hyaluronic acid-based nanosystems for CD44 mediated anti-inflammatory and antinociceptive activity. *Int J Mol Sci*. 2023;24(8):7286. doi:10.3390/ijms24087286
40. Park D, Kim Y, Kim H, et al. Hyaluronic acid promotes angiogenesis by inducing RHAMM-TGFbeta receptor interaction via CD44-PKCdelta. *Mol Cells*. 2012;33(6):563–574. doi:10.1007/s10059-012-2294-1
41. Tolg C, Liu M, Cousteils K, et al. Cell-specific expression of the transcriptional regulator RHAMM provides a timing mechanism that controls appropriate wound re-epithelialization. *J Biol Chem*. 2020;295(16):5427–5448. doi:10.1074/jbc.RA119.010002
42. Fan Y, Choi TH, Chung JH, Jeon YK, Kim S. Hyaluronic acid-cross-linked filler stimulates collagen type 1 and elastic fiber synthesis in skin through the TGF-β/Smad signaling pathway in a nude mouse model. *J Plast Reconstr Aesthet Surg*. 2019;72(8):1355–1362. doi:10.1016/j.bjps.2019.03.032
43. Agarwal G, Agiwal S, Srivastava A. Hyaluronic acid containing scaffolds ameliorate stem cell function for tissue repair and regeneration. *Int J Biol Macromol*. 2020;165(Pt A):388–401. doi:10.1016/j.ijbiomac.2020.09.107
44. Saravanakumar K, Park S, Santosh SS, et al. Application of hyaluronic acid in tissue engineering, regenerative medicine, and nanomedicine: a review. *Int J Biol Macromol*. 2022;222(Pt B):2744–2760. doi:10.1016/j.ijbiomac.2022.10.055
45. Deepak B, Ashley S, Daniel B, Jonathan A. Smoldering subcutaneous polymicrobial infection concealed beneath a cast and a skin graft: delayed wound healing due to recurring soft-tissue infections. *Southwest Respir Crit Care Chron*. 2021;9(37). doi:10.12746/swrccc.v9i37.745

46. Baek W, Lee N, Han EJ, Roh TS, Lee WJ. A prospective randomized study: the usefulness and efficacy of negative pressure wound therapy with lipidocolloid polyester mesh compared to traditional negative pressure wound therapy for treatment of pressure ulcers. *Pharmaceutics*. 2020;12(9):813. doi:10.3390/pharmaceutics12090813
47. Vieceli AS, Martins JC, Hendler KG, et al. Effectiveness of electrophysical agents for treating pressure injuries: a systematic review. *Lasers Med Sci*. 2022;37(9):3363–3377. doi:10.1007/s10103-022-03648-3
48. Sorrell JM, Caplan AI. Topical delivery of mesenchymal stem cells and their function in wounds. *Stem Cell Res Ther*. 2010;1(4):30. doi:10.1186/scrt30
49. Karp JM, Leng Teo GS. Mesenchymal stem cell homing: the devil is in the details. *Cell Stem Cell*. 2009;4(3):206–216. doi:10.1016/j.stem.2009.02.001
50. Garg RK, Rennert RC, Duscher D, et al. Capillary force seeding of hydrogels for adipose-derived stem cell delivery in wounds. *Stem Cells Transl Med*. 2014;3(9):1079–1089. doi:10.5966/sctm.2014-0007
51. Lin CW, Chen YK, Tang KC, Yang KC, Cheng NC, Yu J. Keratin scaffolds with human adipose stem cells: physical and biological effects toward wound healing. *J Tissue Eng Regen Med*. 2019;13(6):1044–1058. doi:10.1002/term.2855
52. Feldman DS, McCauley JF. Mesenchymal stem cells and transforming growth factor-beta(3) (TGF-beta(3)) to enhance the regenerative ability of an albumin scaffold in full thickness wound healing. *J Funct Biomater*. 2018;9(4):65. doi:10.3390/jfb9040065
53. Kilic Bektas C, Kimiz I, Sendemir A, Hasirci V, Hasirci N. A bilayer scaffold prepared from collagen and carboxymethyl cellulose for skin tissue engineering applications. *J Biomater Sci Polym Ed*. 2018;29(14):1764–1784. doi:10.1080/09205063.2018.1498718
54. Ribeiro J, Pereira T, Amorim I, et al. Cell therapy with human MSCs isolated from the umbilical cord Wharton jelly associated to a PVA membrane in the treatment of chronic skin wounds. *Int J Med Sci*. 2014;11(10):979–987. doi:10.7150/ijms.9139
55. Kakehi K, Kinoshita M, Yasueda S. Hyaluronic acid: separation and biological implications. *J Chromatogr B Analyt Technol Biomed Life Sci*. 2003;797(1–2):347–355. doi:10.1016/s1570-0232(03)00479-3
56. Kim H, Jeong H, Han S, et al. Hyaluronate and its derivatives for customized biomedical applications. *Biomaterials*. 2017;123:155–171. doi:10.1016/j.biomaterials.2017.01.029
57. Prestwich GD. Hyaluronic acid-based clinical biomaterials derived for cell and molecule delivery in regenerative medicine. *J Control Release*. 2011;155(2):193–199. doi:10.1016/j.jconrel.2011.04.007
58. Aleksander-Konert E, Paduszynski P, Zajdel A, Dzierzewicz Z, Wilczok A. In vitro chondrogenesis of Wharton's jelly mesenchymal stem cells in hyaluronic acid-based hydrogels. *Cell Mol Biol Lett*. 2016;21:11. doi:10.1186/s11658-016-0016-y
59. Lopez-Ruiz E, Jimenez G, Alvarez de Cienfuegos L, et al. Advances of hyaluronic acid in stem cell therapy and tissue engineering, including current clinical trials. *Eur Cell Mater*. 2019;37:186–213. doi:10.22203/eCM.v037a12
60. Alemzadeh E, Oryan A, Mohammadi AA. Hyaluronic acid hydrogel loaded by adipose stem cells enhances wound healing by modulating IL-1beta, TGF-beta1, and bFGF in burn wound model in rat. *J Biomed Mater Res B Appl Biomater*. 2020;108(2):555–567. doi:10.1002/jbm.b.34411
61. Hu W, Zhu S, Fanai ML, Wang J, Cai J, Feng J. 3D co-culture model of endothelial colony-forming cells (ECFCs) reverses late passage adipose-derived stem cell senescence for wound healing. *Stem Cell Res Ther*. 2020;11(1):355. doi:10.1186/s13287-020-01838-w
62. Pak CS, Heo CY, Shin J, Moon SY, Cho SW, Kang HJ. Effects of a catechol-functionalized hyaluronic acid patch combined with human adipose-derived stem cells in diabetic wound healing. *Int J Mol Sci*. 2021;22(5):2632. doi:10.3390/ijms22052632
63. Stadler I, Zhang RY, Oskoui P, Whittaker MS, Lanzafame RJ. Development of a simple, noninvasive, clinically relevant model of pressure ulcers in the mouse. *J Invest Surg*. 2004;17(4):221–227. doi:10.1080/08941930490472046
64. Saito Y, Hasegawa M, Fujimoto M, et al. The loss of MCP-1 attenuates cutaneous ischemia-reperfusion injury in a mouse model of pressure ulcer. *J Invest Dermatol*. 2008;128(7):1838–1851. doi:10.1038/sj.jid.5701258
65. Motegi SI, Sekiguchi A, Uchiyama A, et al. Protective effect of mesenchymal stem cells on the pressure ulcer formation by the regulation of oxidative and endoplasmic reticulum stress. *Sci Rep*. 2017;7(1):17186. doi:10.1038/s41598-017-17630-5
66. Sekiguchi A, Motegi SI, Uchiyama A, et al. Botulinum toxin B suppresses the pressure ulcer formation in cutaneous ischemia-reperfusion injury mouse model: possible regulation of oxidative and endoplasmic reticulum stress. *J Dermatol Sci*. 2018;90(2):144–153. doi:10.1016/j.jdermsci.2018.01.006
67. Xiao S, Xiao C, Miao Y, et al. Human acellular amniotic membrane incorporating exosomes from adipose-derived mesenchymal stem cells promotes diabetic wound healing. *Stem Cell Res Ther*. 2021;12(1):255. doi:10.1186/s13287-021-02333-6
68. Ebrahim N, Dessouky AA, Mostafa O, et al. Adipose mesenchymal stem cells combined with platelet-rich plasma accelerate diabetic wound healing by modulating the Notch pathway. *Stem Cell Res Ther*. 2021;12(1):392. doi:10.1186/s13287-021-02454-y
69. Yoon D, Yoon D, Sim H, Hwang I, Lee JS, Chun W. Accelerated wound healing by fibroblasts differentiated from human embryonic stem cell-derived mesenchymal stem cells in a pressure ulcer animal model. *Stem Cells Int*. 2018;2018:4789568. doi:10.1155/2018/4789568
70. Dong Y, Cui M, Qu J, et al. Conformable hyaluronic acid hydrogel delivers adipose-derived stem cells and promotes regeneration of burn injury. *Acta Biomater*. 2020;108:56–66. doi:10.1016/j.actbio.2020.03.040
71. Jiao W, Mi X, Yang Y, et al. Mesenchymal stem cells combined with autocrosslinked hyaluronic acid improve mouse ovarian function by activating the PI3K-AKT pathway in a paracrine manner. *Stem Cell Res Ther*. 2022;13(1):49. doi:10.1186/s13287-022-02724-3
72. Zhang Z, Shao M, Hepler C, et al. Dermal adipose tissue has high plasticity and undergoes reversible dedifferentiation in mice. *J Clin Invest*. 2019;129(12):5327–5342. doi:10.1172/JCI130239
73. Shook BA, Wasko RR, Mano O, et al. Dermal adipocyte lipolysis and myofibroblast conversion are required for efficient skin repair. *Cell Stem Cell*. 2020;26(6):880–895e6. doi:10.1016/j.stem.2020.03.013
74. Jin CE, Xiao L, Ge ZH, Zhan XB, Zhou HX. Role of adiponectin in adipose tissue wound healing. *Genet Mol Res*. 2015;14(3):8883–8891. doi:10.4238/2015.August.3.11
75. Salathia NS, Shi J, Zhang J, Glynne RJ. An in vivo screen of secreted proteins identifies adiponectin as a regulator of murine cutaneous wound healing. *J Invest Dermatol*. 2013;133(3):812–821. doi:10.1038/jid.2012.374
76. Shibata S, Tada Y, Asano Y, et al. Adiponectin regulates cutaneous wound healing by promoting keratinocyte proliferation and migration via the ERK signaling pathway. *J Immunol*. 2012;189(6):3231–3241. doi:10.4049/jimmunol.1101739

77. Frank S, Stallmeyer B, Kampfer H, Kolb N, Pfeilschifter J. Leptin enhances wound re-epithelialization and constitutes a direct function of leptin in skin repair. *J Clin Invest*. 2000;106(4):501–509. doi:10.1172/JCI9148
78. Ring BD, Scully S, Davis CR, et al. Systemically and topically administered leptin both accelerate wound healing in diabetic ob/ob mice. *Endocrinology*. 2000;141(1):446–449. doi:10.1210/endo.141.1.7373
79. Schmidt BA, Horsley V. Intradermal adipocytes mediate fibroblast recruitment during skin wound healing. *Development*. 2013;140(7):1517–1527. doi:10.1242/dev.087593
80. Zeve D, Tang W, Graff J. Fighting fat with fat: the expanding field of adipose stem cells. *Cell Stem Cell*. 2009;5(5):472–481. doi:10.1016/j.stem.2009.10.014
81. Wang J, Cai J, Zhang Q, Wen J, Liao Y, Lu F. Fat transplantation induces dermal adipose regeneration and reverses skin fibrosis through dedifferentiation and redifferentiation of adipocytes. *Stem Cell Res Ther*. 2022;13(1):499. doi:10.1186/s13287-022-03127-0
82. Tan QW, Tang SL, Zhang Y, et al. Hydrogel from acellular porcine adipose tissue accelerates wound healing by inducing intradermal adipocyte regeneration. *J Invest Dermatol*. 2019;139(2):455–463. doi:10.1016/j.jid.2018.08.013
83. Borel V, Gallot D, Marceau G, Sapin V, Blanchon L. Placental implications of peroxisome proliferator-activated receptors in gestation and parturition. *PPAR Res*. 2008;2008:758562. doi:10.1155/2008/758562
84. Chen M, Jing D, Ye R, Yi J, Zhao Z. PPARbeta/delta accelerates bone regeneration in diabetic mellitus by enhancing AMPK/mTOR pathway-mediated autophagy. *Stem Cell Res Ther*. 2021;12(1):566. doi:10.1186/s13287-021-02628-8
85. Escher P, Wahli W. Peroxisome proliferator-activated receptors: insight into multiple cellular functions. *Mutat Res*. 2000;448(2):121–138. doi:10.1016/s0027-5107(99)00231-6
86. Mirza AZ, Althagafi II, Shamshad H. Role of PPAR receptor in different diseases and their ligands: physiological importance and clinical implications. *Eur J Med Chem*. 2019;166:502–513. doi:10.1016/j.ejmech.2019.01.067
87. Lefebvre P, Chinetti G, Fruchart JC, Staels B. Sorting out the roles of PPAR alpha in energy metabolism and vascular homeostasis. *J Clin Invest*. 2006;116(3):571–580. doi:10.1172/JCI27989
88. Yu S, Rao S, Reddy JK. Peroxisome proliferator-activated receptors, fatty acid oxidation, steatohepatitis and hepatocarcinogenesis. *Curr Mol Med*. 2003;3(6):561–572. doi:10.2174/1566524033479537
89. Goya K, Sumitani S, Xu X, et al. Peroxisome proliferator-activated receptor alpha agonists increase nitric oxide synthase expression in vascular endothelial cells. *Arterioscler Thromb Vasc Biol*. 2004;24(4):658–663. doi:10.1161/01.ATV.0000118682.58708.78
90. Marx N, Mackman N, Schonbeck U, et al. PPARalpha activators inhibit tissue factor expression and activity in human monocytes. *Circulation*. 2001;103(2):213–219. doi:10.1161/01.cir.103.2.213
91. Wojtowicz S, Strosznajder AK, Jezyna M, Strosznajder JB. The Novel Role of PPAR alpha in the brain: promising target in therapy of alzheimer's disease and other neurodegenerative disorders. *Neurochem Res*. 2020;45(5):972–988. doi:10.1007/s11064-020-02993-5
92. Shibasaki M, Takahashi K, Itou T, Bujo H, Saito Y. A PPAR agonist improves TNF-alpha-induced insulin resistance of adipose tissue in mice. *Biochem Biophys Res Commun*. 2003;309(2):419–424. doi:10.1016/j.bbrc.2003.07.007
93. Gurnell M, Wentworth JM, Agostini M, et al. A dominant-negative peroxisome proliferator-activated receptor gamma (PPARgamma) mutant is a constitutive repressor and inhibits PPARgamma-mediated adipogenesis. *J Biol Chem*. 2000;275(8):5754–5759. doi:10.1074/jbc.275.8.5754
94. Ali AT, Hochfeld WE, Myburgh R, Pepper MS. Adipocyte and adipogenesis. *Eur J Cell Biol*. 2013;92(6–7):229–236. doi:10.1016/j.ejcb.2013.06.001
95. Magadum A, Engel FB. PPARbeta/delta: linking Metabolism to Regeneration. *Int J Mol Sci*. 2018;19(7). doi:10.3390/ijms19072013
96. Berger J, Moller DE. The mechanisms of action of PPARs. *Annu Rev Med*. 2002;53:409–435. doi:10.1146/annurev.med.53.082901.104018
97. Abbott BD. Review of the expression of peroxisome proliferator-activated receptors alpha (PPAR alpha), beta (PPAR beta), and gamma (PPAR gamma) in rodent and human development. *Reprod Toxicol*. 2009;27(3–4):246–257. doi:10.1016/j.reprotox.2008.10.001
98. Di-Poi N, Tan NS, Michalik L, Wahli W, Desvergne B. Antiapoptotic role of PPARbeta in keratinocytes via transcriptional control of the Akt1 signaling pathway. *Mol Cell*. 2002;10(4):721–733. doi:10.1016/s1097-2765(02)00646-9
99. Tan NS, Michalik L, Di-Poi N, Desvergne B, Wahli W. Critical roles of the nuclear receptor PPARbeta (peroxisome-proliferator-activated receptor beta) in skin wound healing. *Biochem Soc Trans*. 2004;32(Pt 1):97–102. doi:10.1042/bst0320097
100. Tan NS, Icre G, Montagner A, Bordier-ten-Heggeler B, Wahli W, Michalik L. The nuclear hormone receptor peroxisome proliferator-activated receptor beta/delta potentiates cell chemotactism, polarization, and migration. *Mol Cell Biol*. 2007;27(20):7161–7175. doi:10.1128/MCB.00436-07
101. Han JK, Lee HS, Yang HM, et al. Peroxisome proliferator-activated receptor-delta agonist enhances vasculogenesis by regulating endothelial progenitor cells through genomic and nongenomic activations of the phosphatidylinositol 3-kinase/Akt pathway. *Circulation*. 2008;118(10):1021–1033. doi:10.1161/CIRCULATIONAHA.108.777169
102. Piqueras L, Reynolds AR, Hodivala-Dilke KM, et al. Activation of PPARbeta/delta induces endothelial cell proliferation and angiogenesis. *Arterioscler Thromb Vasc Biol*. 2007;27(1):63–69. doi:10.1161/01.ATV.0000250972.83623.61
103. Chong HC, Chan JS, Goh CQ, et al. Angiopoietin-like 4 stimulates STAT3-mediated iNOS expression and enhances angiogenesis to accelerate wound healing in diabetic mice. *Mol Ther*. 2014;22(9):1593–1604. doi:10.1038/mt.2014.102
104. Goh YY, Pal M, Chong HC, et al. Angiopoietin-like 4 interacts with matrix proteins to modulate wound healing. *J Biol Chem*. 2010;285(43):32999–33009. doi:10.1074/jbc.M110.108175
105. Bornstein P, Sage EH. Matricellular proteins: extracellular modulators of cell function. *Curr Opin Cell Biol*. 2002;14(5):608–616. doi:10.1016/s0955-0674(02)00361-7
106. Fernandez-Hernando C, Suarez Y. ANGPTL4: a multifunctional protein involved in metabolism and vascular homeostasis. *Curr Opin Hematol*. 2020;27(3):206–213. doi:10.1097/MOH.0000000000000580
107. Stoimenov I, Helleday T. PCNA on the crossroad of cancer. *Biochem Soc Trans*. 2009;37(Pt 3):605–613. doi:10.1042/BST0370605
108. Bainbridge P. Wound healing and the role of fibroblasts. *J Wound Care*. 2013;22(8):407–8, 410–12. doi:10.12968/jowc.2013.22.8.407
109. Pan Y, Lin T, Shao L, et al. Lignin/puerarin nanoparticle-incorporated hydrogel improves angiogenesis through puerarin-induced autophagy activation. *Int J Nanomed*. 2023;18:5095–5117. doi:10.2147/IJN.S412835
110. Ren H, Su P, Zhao F, et al. Adipose mesenchymal stem cell-derived exosomes promote skin wound healing in diabetic mice by regulating epidermal autophagy. *Burns Trauma*. 2024;12:tkae001. doi:10.1093/burnst/tkae001

111. Tobita Y, Arima T, Nakano Y, Uchiyama M, Shimizu A, Takahashi H. Peroxisome proliferator-activated receptor beta/delta agonist suppresses inflammation and promotes neovascularization. *Int J Mol Sci*. 2020;21(15):5296. doi:10.3390/ijms21155296
112. Chong HC, Tan MJ, Philippe V, et al. Regulation of epithelial-mesenchymal IL-1 signaling by PPARbeta/delta is essential for skin homeostasis and wound healing. *J Cell Biol*. 2009;184(6):817–831. doi:10.1083/jcb.200809028
113. Wang X, Sng MK, Foo S, et al. Early controlled release of peroxisome proliferator-activated receptor beta/delta agonist GW501516 improves diabetic wound healing through redox modulation of wound microenvironment. *J Control Release*. 2015;197:138–147. doi:10.1016/j.jconrel.2014.11.001
114. Bonnici L, Suleiman S, Schembri-Wismayer P, Cassar A. Targeting signalling pathways in chronic wound healing. *Int J Mol Sci*. 2023;25(1). doi:10.3390/ijms25010050
115. Ginouves A, Ilc K, Macias N, Pouyssegur J, Berra E. PHDs overactivation during chronic hypoxia "desensitizes" HIFalpha and protects cells from necrosis. *Proc Natl Acad Sci U S A*. 2008;105(12):4745–4750. doi:10.1073/pnas.0705680105
116. Sulkshane P, Ram J, Thakur A, Reis N, Kleifeld O, Glickman MH. Ubiquitination and receptor-mediated mitophagy converge to eliminate oxidation-damaged mitochondria during hypoxia. *Redox Biol*. 2021;45:102047. doi:10.1016/j.redox.2021.102047
117. Smith RA, Hartley RC, Cocheme HM, Murphy MP. Mitochondrial pharmacology. *Trends Pharmacol Sci*. 2012;33(6):341–352. doi:10.1016/j.tips.2012.03.010
118. Bensellam M, Maxwell EL, Chan JY, et al. Hypoxia reduces ER-to-Golgi protein trafficking and increases cell death by inhibiting the adaptive unfolded protein response in mouse beta cells. *Diabetologia*. 2016;59(7):1492–1502. doi:10.1007/s00125-016-3947-y
119. Kosol W, Kumar S, Marrero-BerrIos I, Berthiaume F. Medium conditioned by human mesenchymal stromal cells reverses low serum and hypoxia-induced inhibition of wound closure. *Biochem Biophys Res Commun*. 2020;522(2):335–341. doi:10.1016/j.bbrc.2019.11.071
120. Liao C, Liu Y, Lin Y, Wang J, Zhou T, Weng W. Mesenchymal stem cell-conditioned medium protecting renal tubular epithelial cells by inhibiting hypoxia-inducible factor-1alpha and nuclear receptor coactivator-1. *Curr Stem Cell Res Ther*. 2024;19(10):1369–1381. doi:10.2174/011574888X247652230928064627
121. Aguilar-Recarte D, Barroso E, Guma A, et al. GDF15 mediates the metabolic effects of PPARbeta/delta by activating AMPK. *Cell Rep*. 2021;36(6):109501. doi:10.1016/j.celrep.2021.109501
122. Papatheodorou I, Makrecka-Kuka M, Kuka J, Liepinsh E, Dambrova M, Lazou A. Pharmacological activation of PPARbeta/delta preserves mitochondrial respiratory function in ischemia/reperfusion via stimulation of fatty acid oxidation-linked respiration and PGC-1alpha/NRF-1 signaling. *Front Endocrinol*. 2022;13:941822. doi:10.3389/fendo.2022.941822
123. Inoue T, Kohro T, Tanaka T, et al. Cross-enhancement of ANGPTL4 transcription by HIF1 alpha and PPAR beta/delta is the result of the conformational proximity of two response elements. *Genome Biol*. 2014;15(4):R63. doi:10.1186/gb-2014-15-4-r63
124. Hsu LC, Peng BY, Chen MS, et al. The potential of the stem cells composite hydrogel wound dressings for promoting wound healing and skin regeneration: in vitro and in vivo evaluation. *J Biomed Mater Res B Appl Biomater*. 2019;107(2):278–285. doi:10.1002/jbm.b.34118
125. Gao T, Tian C, Ma Z, Chu Z, Wang Z, Zhang P. Stem cell seeded and silver nanoparticles loaded bilayer PLGA/PVA dressings for wound healing. *Macromol Biosci*. 2020;20(10):e2000141. doi:10.1002/mabi.202000141
126. Yu Q, Sun H, Yue Z, et al. Zwitterionic polysaccharide-based hydrogel dressing as a stem cell carrier to accelerate burn wound healing. *Adv Healthc Mater*. 2023;12(7):e2202309. doi:10.1002/adhm.202202309
127. Moon KC, Suh HS, Kim KB, et al. Potential of allogeneic adipose-derived stem cell-hydrogel complex for treating diabetic foot ulcers. *Diabetes*. 2019;68(4):837–846. doi:10.2337/db18-0699